

Trachyandesite of Kennedy Table, its vent complex, and post–9.3 Ma uplift of the central Sierra Nevada

present-day basal gradients of several were

adjusted for apparent dip and projected

along a vertical plane at 220° (the estimated

tilt azimuth). The basal gradients are far

steeper than that of the modern river, but

they differ slightly from reach to reach and

are thus inconsistent measures of the post-

Miocene tilt. Likewise, relief eroded atop

most remnants renders modeling of upper

surfaces suspect. At Little Dry Creek, how-

ever, a chain of nine remnants rests on fluvial

floodplain sand and gravel; this chain trends

230°, and its smooth basal contact now dips

1.36° (adjusted at 220°). Projection of this

dip 89 km from the 207 m base of the most

distal remnant at Little Dry Creek to the vent

intrusion falls far below the 2760 m intru-

sion-to-lava-flow transition near the Sierran

crest, showing that the Sierran block has not

undergone pronounced convex warping. Us-

ing elevation data on paleoriver meanders

preserved by the lava flow, we show that the

paleogradient has a cosine dependence on

meander-section azimuth, indicating tilting.

Subtraction of 1.07° of dip restores the data

to an azimuth-independent configuration, in-

dicating total tilting since 9.3 Ma of 1.07° and

an original large-scale gradient of 0.46°, simi-

lar to the published value of 0.33° at Squaw

Leap, but larger than the previously obtained

value of 0.057° at Little Dry Creek. Subtrac-

tion of those Miocene estimates from the ob-

servable 1.643° tilt along the section from Lit-

tle Dry Creek to the vent yields vent uplift of

2464 m (for 0.057°), 1835 m (for 0.46°), and

2040 m (for 0.33°). Confirmation of earlier

assumptions regarding Miocene river gradi-

ent and block rigidity greatly strengthens the

case for \sim 2 km of late Cenozoic uplift of the

Wes Hildreth^{1,†}, Judy Fierstein¹, Fred M. Phillips², and Andy Calvert¹

¹Volcano Science Center, U.S. Geological Survey, Menlo Park, California 94025, USA ²New Mexico Institute of Mining & Technology, Socorro, New Mexico 87801, USA

ABSTRACT

Tectonic interpretation of the central Sierra Nevada—whether the crest of the Sierra Nevada (California, USA) was uplifted in the late Cenozoic or whether the range has undergone continuous down-wearing since the Late Cretaceous—is controversial, since there is no obvious tectonic explanation for renewed uplift. The strongest direct evidence for late Cenozoic uplift of the central Sierra Nevada comes from study of the Trachyandesite of Kennedy Table, which followed the course of the Miocene San Joaquin River but has a steeper gradient than the modern river. Early workers attributed this steeper gradient to tilting of the Sierra Nevada block since the late Miocene, resulting in 2 km of rangecrest uplift. However, this interpretation has been contested on grounds that the Miocene river gradient had to be assumed and that the Sierran Batholith could have warped during tilting, thus failing to uplift the range crest. The objective of this study was to obtain quantitative data that test these criticisms.

The Trachyandesite of Kennedy Table is a chain of 33 remnants of a single lava flow as thick as 65 m, preserved for 21 km from Squaw Leap to Little Dry Creek, close to the modern San Joaquin River in the foothills of the Sierra Nevada. Several remnants lie on fluvial gravel of the late Miocene San Joaquin River. Early workers speculated that the lava concealed its own (unrecognized) vent, but in 2011, we identified the vent on the Middle Fork of the San Joaquin River, 13.5 km south of Deadman Pass and 70 km northeast of Kennedy Table. The vent complex intrudes Cretaceous granite, has 285 m relief, and is an intricately jointed intrusion that grades up into a glassy lava flow. Composition (58% SiO₂) and ⁴⁰Ar/³⁹Ar age (9.3 Ma) are identical at the vent and downstream. Basal elevations of remnants were recorded, and the

INTRODUCTION

central Sierra Nevada crest.

For nearly 150 yr, the Sierra Nevada has presented a tectonic enigma. The Sierra Nevada batholith was emplaced adjacent to a convergent

boundary, as the root of a volcanic arc, during the Mesozoic (Bateman and Eaton, 1967; Saleeby et al., 2008). Like today's Andes, this arc was elevated and formed the western edge of a high inland plateau (Henry et al., 2012; House et al., 1998; Sharman et al., 2015). Between 90 and 60 Ma, this high range was rapidly eroded down to the level of the roof of the batholith, after which erosion greatly slowed (Cecil et al., 2006; McPhillips and Brandon, 2012). The enigmatic aspect is that ever since the days of the earliest scientific explorers, geologists have described evidence that the range has experienced renewed uplift, and consequent incision, in the late Cenozoic (Christensen, 1966; Le Conte, 1886; Lindgren, 1911; Stock et al., 2004; Wakabayashi, 2013), after the shift from a convergent to a transform boundary. Although crustal thickening and surface uplift are expected at a convergent margin, the origins of renewed uplift following extended postbatholith quiescence are not obvious. Proposed mechanisms include an erosional/ depositional lever driven by accelerated Pleistocene erosion (proposed by Small and Anderson [1995] and evaluated negatively by Jones et al. [2004]), isostatic response to delamination of a dense crustal root of the batholith (Ducea and Saleeby, 1996; Jones et al., 2004; Le Pourhiet et al., 2006), dynamic uplift due to asthenospheric upwelling (Jayko, 2009; Le Pourhiet et al., 2006; Zhou and Liu, 2019), and isostatic response to tectonic unloading on the bounding normal faults on the east side of the range (Martel et al., 2014; Thompson and Parsons, 2009).

An alternative explanation of the renewed-uplift problem is that, in fact, late Cenozoic uplift is illusory. This implies that the Sierra Nevada has maintained its elevation, or decreased in mean elevation, since Oligocene time or earlier, in turn implying that the observed channel gradients of any Cenozoic paleostreams are the original gradients. The reality of late Cenozoic uplift has been contested on a variety of evidence, including evidence for crustal thinning (leading to subsidence) in the late Cenozoic (Wernicke et al., 1996); comparison of early Cenozoic

†hildreth@usgs.gov.

GSA Bulletin;

https://doi.org/10.1130/B36125.1; 8 figures; 1 table; 1 supplemental file.

stable-isotope profiles and other paleoenvironmental indicators with elevation against modern profiles (little difference) (Cassel et al., 2009; Hren et al., 2010; Mix et al., 2016); lack of evidence for deflection of atmospheric circulation by an uplifting orographic barrier (Chamberlain et al., 2012; Mix et al., 2019); and weakness of the geomorphic evidence for uplift (Gabet, 2014). We note that most of this evidence comes from the northern Sierra Nevada, which is currently ~2 km lower in average elevation at the crest than the central/southern Sierra Nevada.

In light of these conflicting interpretations, it is worthwhile to reassess the direct evidence for late Cenozoic uplift. Although unquestionably pertinent, data such as stable-isotope elevation profiles, crustal thickness, inferred atmospheric circulation, and paleobotany provide only indirect evidence for the presence or absence of uplift. The most direct evidence is provided by geomorphic markers that can be demonstrated to have been formed at one attitude and subsequently tilted to a steeper attitude. In the central Sierra Nevada (which we define as 36.8°N to 38.2°N latitude; South Fork Kings River to Stanislaus River), the linchpin for direct evidence of tilt is Huber's classic 1981 study on the San Joaquin River (Huber, 1981), where he showed that a late Miocene lava flow was tilted $\sim 1.2^{\circ}$ steeper than corresponding portions of the modern river. Extrapolating this to the range crest, he estimated \sim 2 km of uplift there. Although the study was thorough and the evidence strong, Gabet (2014) leveled two salient criticisms: (1) Lacking data, Huber was forced to assume that the gradient of the Miocene river had been similar to the modern one, an assumption that could be erroneous, and (2) in order to estimate crestal uplift, Huber had to assume that the range tilted as a rigid block, an assumption that Gabet termed "unlikely." Huber (1981) had also acknowledged these weaknesses. In this study, we focused on addressing these two criticisms of Huber's analysis of the tilt of the San Joaquin River drainage. We accomplished this (1) by locating the vent from which Huber's lava flow, the Trachyandesite of Kennedy Table, was erupted, and (2) by quantifying the depositional gradient of the Miocene river through geometric analysis of the gradient along the course of meanders traced by the flow.

The late Miocene Trachyandesite of Kennedy Table is preserved as a set of 33 remnants of a voluminous lava flow as thick as 65 m, scattered for 21–23 km along both sides of the modern San Joaquin River above Friant Dam (Fig. 1), where the river passes from the Sierra Nevada into the Central Valley of California (Macdonald, 1941; Bateman and Busacca, 1982). The flow rests either directly on Mesozoic tonalitic basement or on 30–60 m of intervening Miocene

fluvial gravels of the paleo—San Joaquin River. Because gradients defined by the bases of its remnants are conspicuously steeper than that of the modern river, the lava flow has been widely cited as a tilted marker (Wahrhaftig, 1965; Christensen, 1966; Bateman and Wahrhaftig, 1966; Small and Anderson, 1995; Wakabayashi, 2013; most analytically by Huber, 1981).

Huber (1981) favored tilting of a rigid (unfaulted, nonwarped) Sierran block. He adopted a 220° tilt azimuth, defined a hinge line at the margin of the Central Valley, estimated a present-day slope of ~1.28° for the most distal remnants, and inferred very low gradients for the Miocene riverbed overrun by the lava flow. With these conditions, he estimated 1.22° of post-lava-flow tilt, which, projected 100 km northeastward to the Sierran range crest, yields 2150 m of uplift at the site of the modern drainage divide. Huber's discussion of alternative models and uncertainties was thorough, and he highlighted the problems in "estimating uplift from profiles reconstructed without some control at the upper end" (Huber, 1981, p. 15). We have now provided that upperend control by locating the eruptive vent on the Middle Fork of the San Joaquin River (hereafter Middle Fork), south of Devils Postpile, 66 km upstream from the nearest lava-flow remnant.

Huber's analysis employed topographic maps at scales of 1:62,500 with 80 ft (24 m) contour intervals. We have been aided by having U.S. Geological Survey (USGS) maps (North American Datum 1927 [NAD 27]) at 1:24,000 scale with contour intervals of 20 ft (6 m) (though intervals are 20 m for the upstream vent complex), as well as data from a pair of handheld field global positioning system (GPS) devices, frequently cross-checked against each other and local bench marks.

Many elevations are cited here in feet to simplify comparison with published topographic maps. Basal contacts of the main lava-flow remnants were recorded in the field with the GPS devices and 20 ft (6 m) contour maps in hand. Where contacts atop gravels or tonalite were exposed, agreement was within a few meters. More widely, the base of the typically steep lava-flow scarp is obscured by its own talus, rendering uncertainty around 5 m (or in a few places as much as 10 m). Because we agree with Huber that the tilt azimuth of the Sierran block is close to 220°, many slopes cited herein were adjusted from apparent dips to true dips in a plane striking perpendicular to 220°.

VENT COMPLEX OF TRACHYANDESITE OF KENNEDY TABLE

Huber speculated that the lava flow had concealed its own vent and had ponded within

a foothills reach only ~23 km long (or allowing for erosion, perhaps a third longer; Huber, 1981, figs. 5 and 6 therein). We located the vent (Fig. 2) for the trachyandesite on the east rim of the Middle Fork, 7.5 km SSW of Mammoth Mountain, 13.5 km south of Deadman Pass, and 84.5 km northeast of Friant Dam. Phenocryst contents and major- and trace-element compositions of the proximal and distal lavas are identical (Table 1). The unit is alkalic intraplate trachyandesite, not arc andesite like that of Miocene Cascadian centers farther north in the Sierra Nevada. Despite repeated searching, we found no remnants of the lava flow along or near the deeply eroded 66-km-long gap between the vent and Bug Table (Fig. 1).

On the left-bank canyon wall of the Middle Fork, the trachyandesite vent complex intrudes Cretaceous granite and is exposed for ~285 m vertically (Fig. 2). The intrusion is exposed for a north-south width of 600 m along the canyon wall, and near the canyon rim, it grades smoothly into a thick lava flow that extends 500 m farther south along the rim (Fig. 2) as well as at least 400 m eastward across the plateau. The granite contact is exposed along the north side of the intrusion all the way to the rim, and the granite still crops out on the plateau as high as the top of the intrusion. The steep face of the intrusion provides no evidence of extrusive facies such as flow breccia or flow contacts. On the face, its original exterior has been eroded, so its ubiquitously intricate jointing (Fig. 3) is internal and is pervasive throughout its vertical exposure. Joint spacing is generally 10-30 cm, and joint setshorizontal, inclined, or vertical-crop out in contiguous domains that are typically 10-20 m across (Fig. 3).

The uppermost \sim 30 m section is partly glassy lava that rims the cliff, extends south along the rim (Fig. 2), and also crops out for 400 m east across the adjacent upland plateau to an elevation as high as 2805 m, where it is overlapped by late Pleistocene lavas (Hildreth and Fierstein, 2016). The intrusive-extrusive transition is imperceptible, but the lava surface is glassier than the intrusion, and its jointing is more polygonal (though not columnar). It seems likely that the intrusive-extrusive transition (at \sim 2760 m or higher) approximates the elevation of the Middle Fork valley at 9.3 Ma, the 40 Ar/ 39 Ar age determined for samples at the vent and distally (Hildreth and Fierstein, 2016).

Relations between the intrusion and its granite host show that there was no canyon here in the late Miocene, just a broad valley. The near-vent trachyandesite surface is 300–600 m lower than the modern drainage divide along Mammoth Crest, just 5 km to its northeast, but it is at nearly the same elevation as a former range-crest saddle

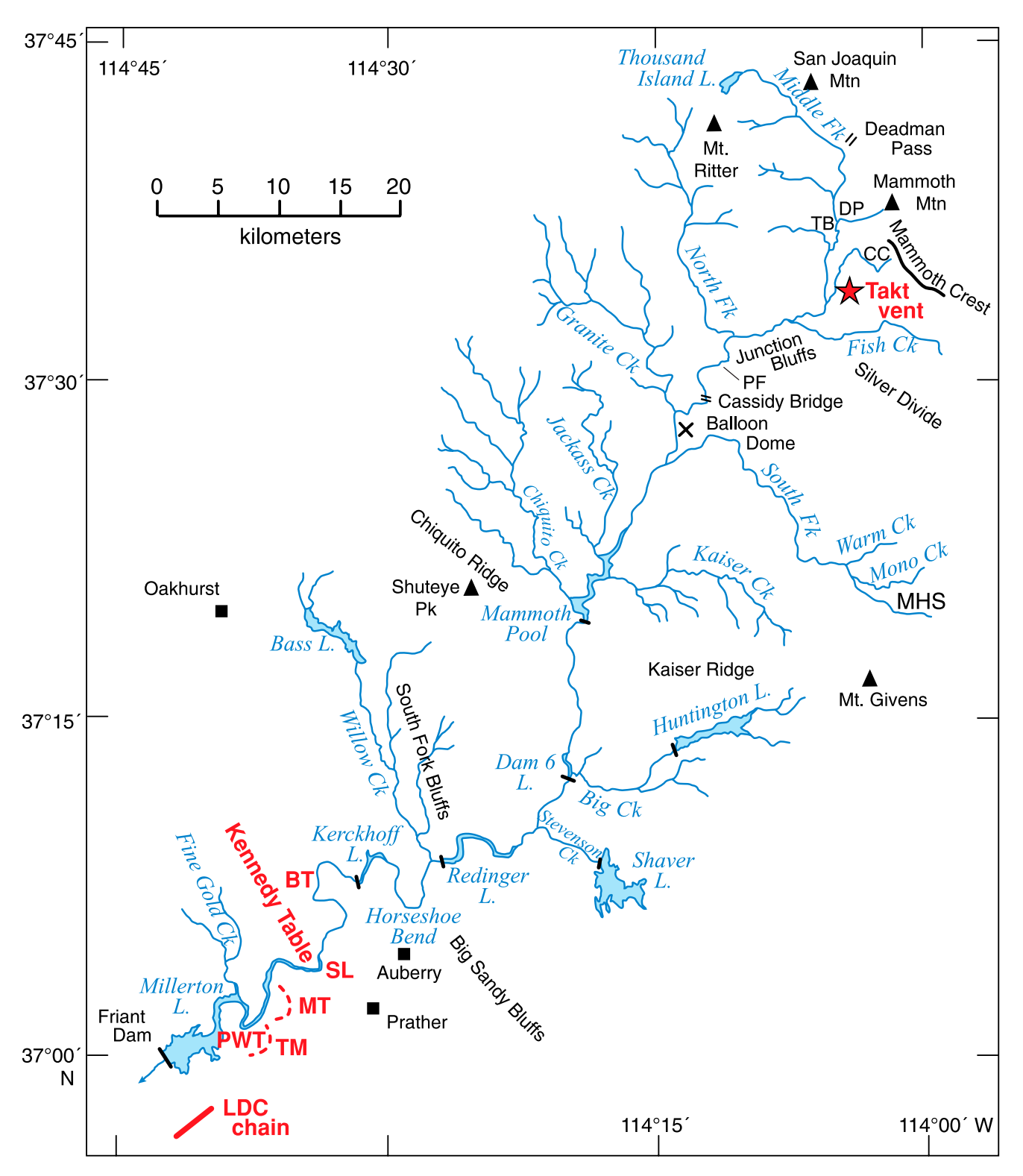


Figure 1. San Joaquin River in Sierra Nevada. Trachyandesite of Kennedy Table crops out at its source (Takt vent) between Mammoth Crest and Middle Fork; and far downstream at Kennedy Table, Bug Table (BT), Squaw Leap (SL), McKenzie Table (MT), Table Mountain (TM), Perkins West Table (PWT), and as a chain of remnants near Little Dry Creek (LDC); see Figures 2–5. Elevations: Mammoth Crest 3100–3500 m; Takt vent (top) 2805 m; Fish Creek confluence 1630 m; South Fork confluence 1130 m; Redinger Dam 425 m; Friant Dam spillway 170 m, at margin of California's Central Valley. Location abbreviations: CC—Crater Creek; DP—Devils Postpile; PF—Pine Flat; TB—The Buttresses; MHS—Mono Hot Springs. Feature abbreviations: Ck—Creek; Fk—Fork; L—Lake. Friant Dam is 84.5 km from Takt vent. Most distal Little Dry Creek remnant is 89 km from Takt vent, along 220° tilt azimuth.

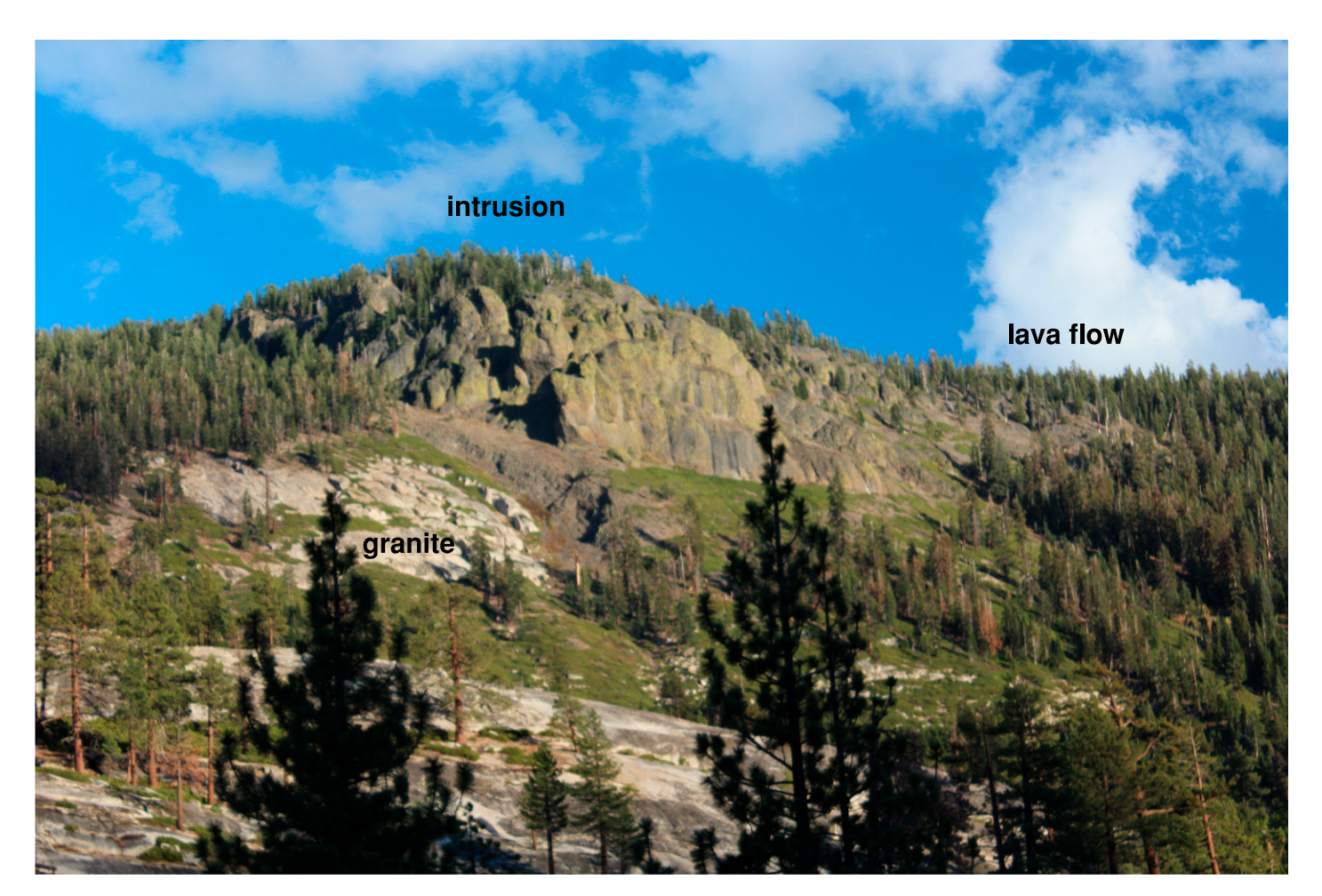


Figure 2. Vent complex of Trachyandesite of Kennedy Table on east wall of Middle Fork San Joaquin River, 6.5 km south of Devils Postpile. Vertical exposure of unit is 285 m, intruding Cretaceous Granite of Mono Creek (in foreground). Obscured in forest at left, granite wall rock remains in contact with the intrusion all the way to the plateau surface. Intrusive mass is as wide as 600 m, but the trachyandesite also extends south (to right) for an additional 500 m as a thick lava flow along the canyon rim. View is eastward from lower Crater Creek.

TABLE 1 CHEMIC	CHANDERITE OF	VENNEDV TADI E

		SiO ₂	TiO ₂	Al ₂ O ₃	FeO*	MnO	MgO	CaO	Na ₂ O	K ₂ O	P ₂ O ₅	Total	Ва	Sr	Rb	Zr	Υ	La	Sc	Ni	Pb	Th
Lava above M-145 M-489	<u>e intrusion</u> Plateau Rim	58.14 57.96	1.06 1.06	18.90 18.96	5.53 5.65	0.09 0.09	2.04 1.98	6.13 6.16	3.75 3.89	3.43 3.36	0.52 0.47	97.48 96.77	1416	971	118	262	23	45	13	10	20	18
Intrusion M-1150 M-1151 M-1151® M-1152	Upper Middle Middle Lower	58.00 58.17 58.17 58.17	1.05 1.06 1.06 1.05	18.94 19.02 19.02 18.93	5.63 5.50 5.50 5.68	0.09 0.09 0.09 0.09	1.99 1.86 1.86 1.96	6.11 6.12 6.12 6.12	3.94 3.85 3.85 3.82	3.37 3.46 3.46 3.31	0.47 0.47 0.47 0.47	98.95 98.62 98.62 98.04	1413 1426 1426 1420	970 972 972 971	118 120 120 117	259 261 261 261	21 21 21 22	45 44 44 46	13 14 14 12	10 9 9 9	21 20 20 20	19 19 19 19
Perkins We M-650 M-650 R M-651	est Table Base Base Top	58.10 58.14 58.10	1.06 1.07 1.06	18.93 18.92 18.84	5.42 5.39 5.57	0.10 0.10 0.09	1.94 1.95 2.04	6.17 6.17 6.16	4.15 4.15 3.96	3.25 3.24 3.30	0.47 0.47 0.47	98.40 99.17 97.83	1491 1503 1401	956 964 952	110 112 121	262 266 263	21 22 22	45 47 44	13 13 12	8 8 7	19 20 20	19 19 19
Squaw Lea M-1004	<u>ap</u> Near base	57.98	1.08	19.09	5.47	0.09	1.78	6.32	4.09	3.22	0.48	97.91	1994	977	105	271	23	49	13	9	19	19
Kennedy T M-1124	<u>able</u> West rim	58.19	1.05	18.90	5.52	0.10	2.00	6.03	3.99	3.36	0.46	98.33	1414	955	117	258	21	44	13	9	21	19
McKenzie M-1006	Lower ledge	57.96	1.07	18.99	5.57	0.10	2.01	6.13	4.09	3.21	0.47	98.81	1476	971	103	272	22	45	13	10	20	19
M-1005	base Upper ledge top	58.07	1.07	18.91	5.60	0.10	2.02	6.15	3.85	3.35	0.47	97.10	1395	953	118	267	22	42	13	8	20	19

Note: X-ray fluorescence (XRF) analyses conducted at Washington State University Geoanalytical Laboratory. Major elements normalized volatile-free to 99.6% total. Major elements in wt%; trace elements in ppm.

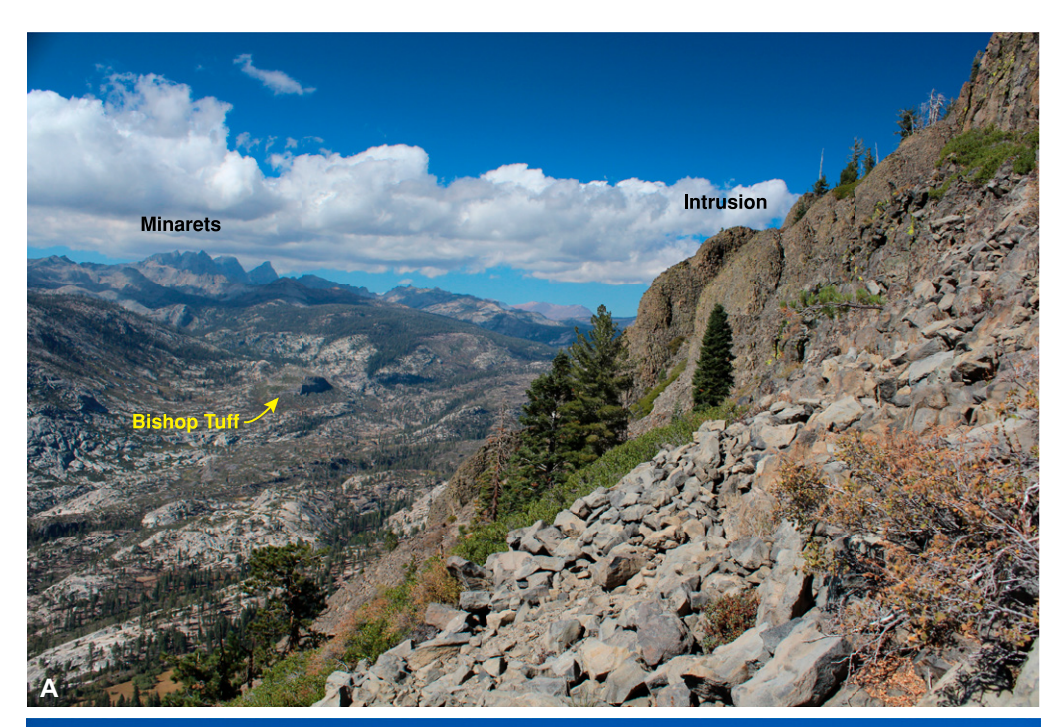




Figure 3. (A) Midslope view of south face of intricately jointed intrusive source of Trachvandesite of Kennedy Table. Granitic floor of Middle Fork is here as much as 400 m lower than lowest exposure of the intrusion and \sim 700 m below its uppermost preserved surface. View is NW to Minarets in Ritter Range on left skyline. Isolated mesa just left of image center is 175-mhigh glaciated remnant of 767 ka Bishop Tuff; its basal contact on granite is 100 m above the modern riverbed and 500 m lower than 9.3 Ma trachyandesite lava flow that issues from the intrusion on canyon rim (Fig. 2). (B) Closer view of south-facing side of lower part of intrusion, illustrating several joint sets of different inclination. Joint spacing is mostly 10-30 cm.

 $\sim\!\!7$ km NNW (now filled by the late Pleistocene Mammoth Mountain volcanic edifice). The intrusion-to-lava transition is today 800 m higher than the floor of the Middle Fork 2 km to the west, but it is also 500 m higher than the floor of the Middle Fork 5.5 km upstream, where the 3.8 Ma Basalt of the Buttresses extends to the present-day granite floor of the canyon (Hildreth and Fierstein, 2016). Most of the incision of the south-flowing reach of the Middle Fork therefore took place between 9.3 and 3.8 Ma.

The trachyandesite surface is also significantly higher than the 2660–2560 m floor of a Pliocene tributary channel of the Middle Fork that had crossed what is now the San Joaquin–Owens River divide just south of Deadman Pass (Fig. 1), 12.5 km north of the trachyandesite vent. The channel was filled and terminated by a 450-m-thick stack of basaltic lavas that erupted between 3.7 and 3.3 Ma (Huber, 1981; Hildreth and Fierstein, 2016). Prior to the closure, rhyolitic and tra-

chydacitic pumice from Miocene ignimbrite eruptions east of the modern divide had been transported along this channel and on down the trunk stream all the way to Little Dry Creek (Fig. 4; see section on fluvial sediments, below). The San Joaquin River is the southernmost of the Sierran rivers shown to have drained in the Miocene across what became the Sierran crestal divide after ca. 3 Ma, in response to Basin and Range extensional faulting (Henry et al., 2012).

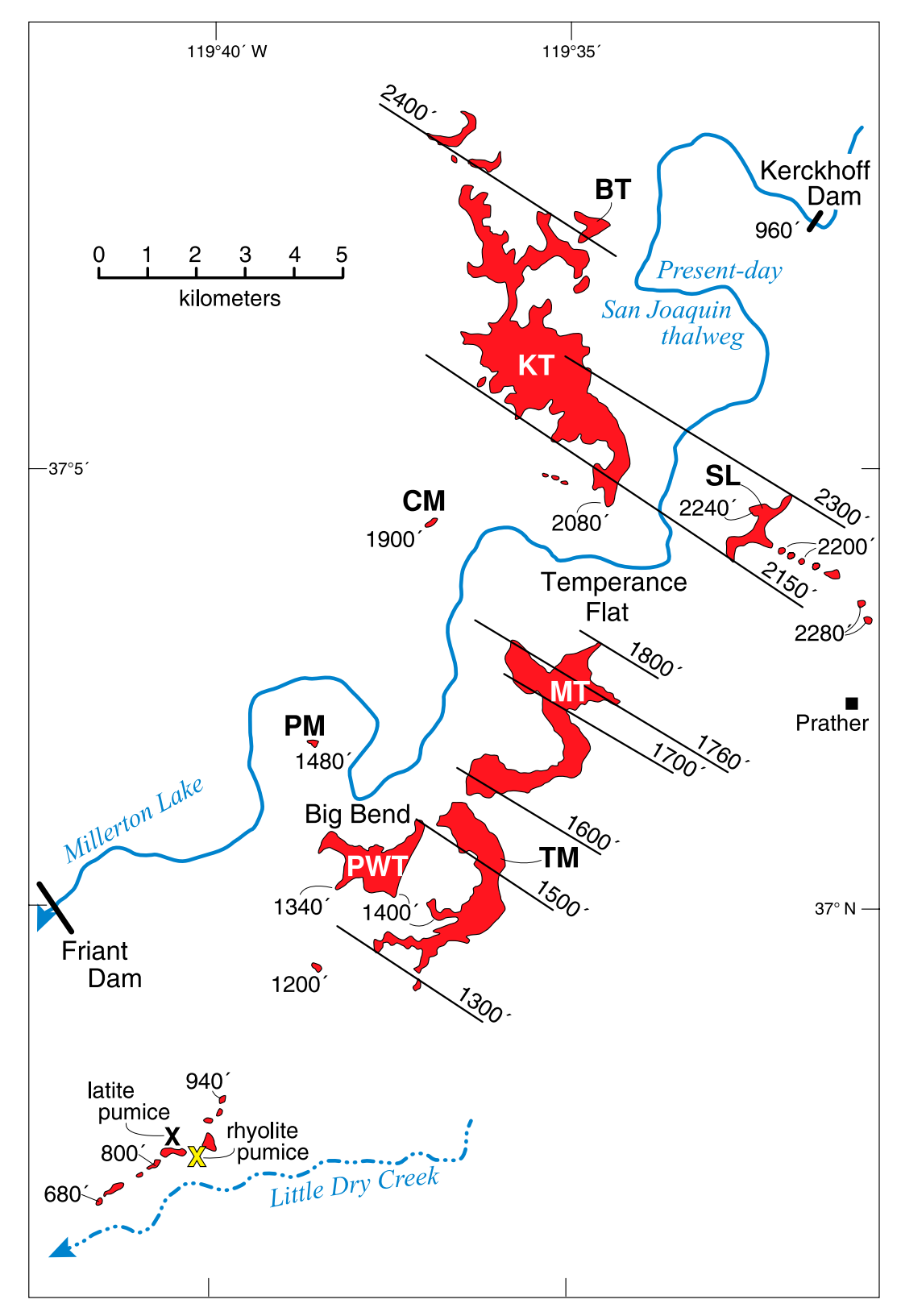


Figure 4. Distribution of 33 remnants of Trachyandesite of Kennedy Table, a single 9.3 Ma lava flow preserved within a 23-km-long swath near the San Joaquin River in the foothills of the Sierra Nevada. Also indicated is meandering channel of modern river, much of which is drowned by Millerton Lake reservoir above Friant Dam. Labeled remnants: BT-Bug Table: CM-Crook Mountain: KT-Kennedy Table; MT-McKenzie Table; PM—Pincushion Mountain; PWT—Perkins West Table; SL—Squaw Leap; TM—Table Mountain; and distal chain near Little Dry Creek (LDC). Elevations are in feet above sea level (as are the 1:24,000 scale topographic maps with 20 ft [6 m] contour intervals used during this study). Contour lines are drawn to connect areas of equal basal elevation along selected stretches where the base is relatively well determined. The contours define a fairly smooth southwest slope of \sim 1.26°. Averaged slope from Squaw Leap to distal Little Dry Creek remnant is 1.37°. Open X, rhyolite pumice, marks fluvially deposited layers of rhyolitic ash and pumice granules intercalated in 46-m-thick section of Miocene gravels beneath the lava-flow remnants at Little Dry Creek. Solid X indicates the layer of latite pumice interbedded in same gravels located and dated by Huber (1981). 1 m = 3.2809 ft.

DOWNSTREAM LAVA FLOW REMNANTS

Among the 33 separate remnants, five are large. The largest is Kennedy Table northwest of the modern river, and Bug Table is

one of its several nearby outliers (Fig. 4). Across the river, the large left-bank remnants (from NE to SW) are tables called Squaw Leap, McKenzie Table (Fig. 5), Table Mountain, and Perkins West Table. A few ki-

lometers farther southwest, a linear chain of nine small remnants that cap a ridge north of Little Dry Creek is the most distal surviving part of the 100-km-long trachyandesite lava flow.

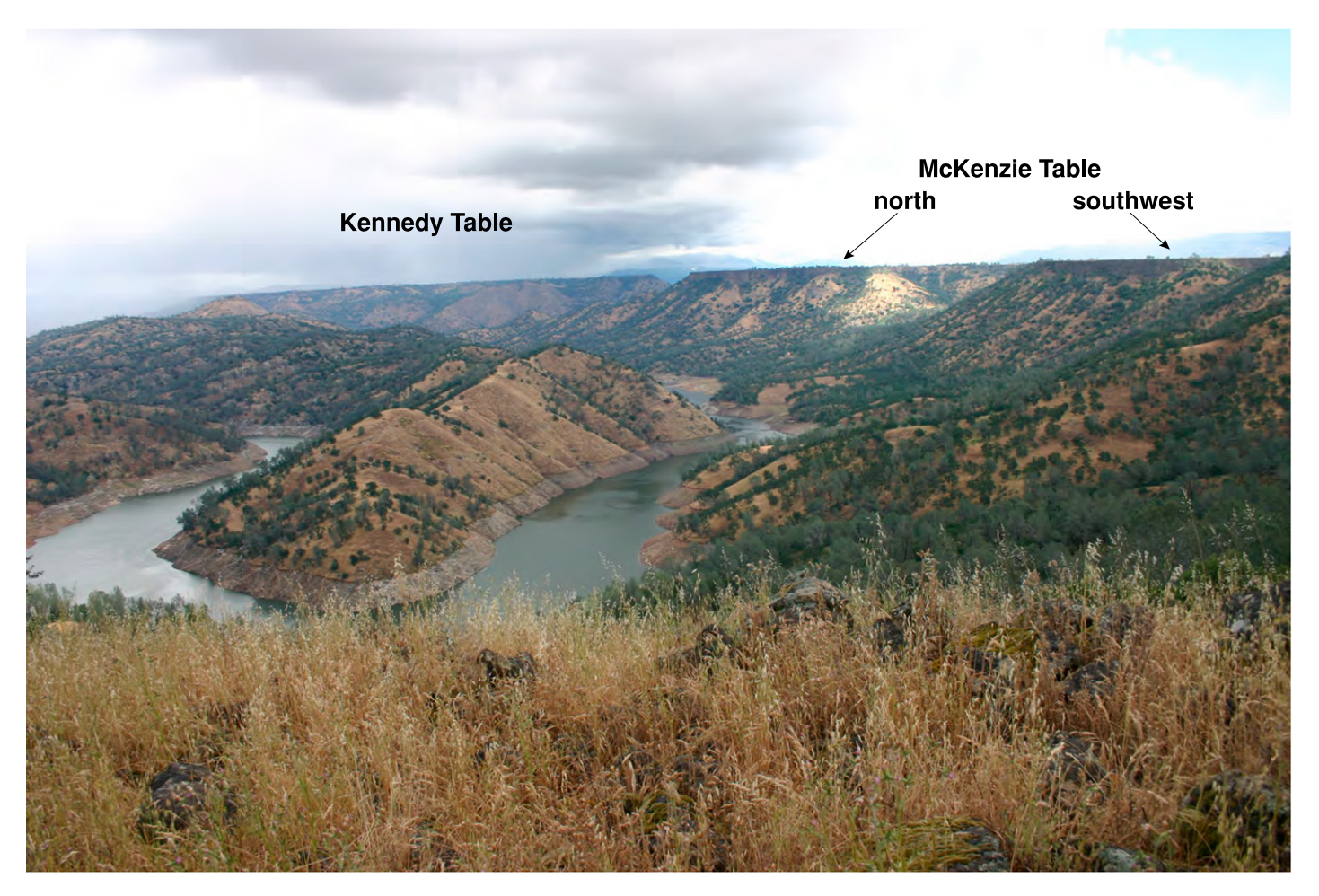


Figure 5. Some downstream remnants of the Trachyandesite of Kennedy Table viewed northeastward from the rim of Perkins West Table. Southwest and north arms of arcuate McKenzie Table (MT) are on right skyline, and south end of Kennedy Table is on left skyline (see Fig. 4). The two tables are separated by a 3.3-km-wide erosional gap where the river bends west through Temperance Flat. Mesa-capping lava flow is here 55–65 m thick. Base of McKenzie Table lava is 320–370 m above surface of Millerton Lake reservoir, which drowns San Joaquin thalweg for at least 25 km upstream from Friant Dam. In left distance, base of south end of Kennedy Table lava is 460 m above the reservoir. At left, Big Bend peninsula is Paleozoic schistose metavolcanic rock, but rocks under the lava flow here are predominantly Cretaceous tonalite (Bateman and Busacca, 1982).

Emplacement of the Lava Flow

Many preserved flow remnants are small and difficult to interpret in terms of original geometry. Others (e.g., Kennedy Table and Perkins West Table) are irregular in outline but appear basically tabular. Two, however, McKenzie Table and Table Mountain, bear a striking resemblance to truncated river meanders. If so, this provides important clues to the configuration of the landscape in the late Miocene. We note, nonetheless, that Huber (1981) interpreted these two tables as "fortuitous" features created by lateral river erosion of a broad, ponded, lava flow. This interpretation was a significant departure from that of earlier geologists, who treated them as filled meanders (Huber, 1981, p. 11). We agree with the earlier workers and think that Huber's explanation of them as accidentally sinuous

remnants of a tabular flow is unlikely for four reasons. First, the shape and amplitude of curvature of McKenzie Table and Table Mountain are quite similar to those of the meanders of the nearby modern San Joaquin River (Fig. 4). The average meander wavelength for the adjacent San Joaquin River is 4.7 ± 0.7 km (7 meanders), and the average amplitude is 2.3 ± 0.7 km. For the tables, the wavelength is 3.7 km, and the amplitude of the preserved portions averages 1.5 km. Complete meanders are not preserved, and so the original amplitude was probably between 1.5 and 3.0 km. As pointed out by Huber (1981), the size of the meanders greatly exceeds that expected for the discharge of the modern San Joaquin River. Based on empirical relations given by Leopold and Wolman (1957), this wavelength should correspond to a river width of \sim 300 m. The actual width of the modern San

Joaquin River varies from \sim 75 m above Millerton Reservoir to \sim 150 m below it. The underfit condition of the modern San Joaquin River is to be expected if both the fossil meanders and the ones followed by the modern river were cut before the large drainage area now east of the Sierra crest was severed by volcanism at 3.7 Ma (Huber, 1981; Hildreth and Fierstein, 2016).

Second, the lateral erosion postulated by Huber would have to be extraordinarily fortuitous to produce these two relatively continuous, winding mesas of approximately constant width that so strongly resemble modern meanders. Third, our analysis (described below) indicates that the flow was emplaced along a topographic gradient similar to that of the modern river, which rules out a ponded flow, as does the gradient of the linear chain of remnants at Little Dry Creek 4–8 km farther southwest. Fourth, although remnants of

the flow cover a large area, most of them are underlain by bedrock. Channel gravels are strictly limited to the meandering reaches at McKenzie Table and Table Mountain and then downstream to Perkins West Table and Little Dry Creek. This suggests that the preserved paleomeanders represent the original thalweg, not later erosional features incised randomly into a broad lava plain.

McKenzie Table and Table Mountain represent strongly inverted topography. During the Miocene, the trachyandesite clearly flowed down the low points in the landscape, but today, the flow is perched 200-400 m above the surrounding land surface. The flow is widely 50-60 m thick and rests on 40-50 m of fluvial gravels. The surrounding landscape is uniformly lower in elevation than these two tables, with the nearest extensive highlands at greater elevation being ~ 10 km to the north and south. We infer that during the late Miocene, the river flowed in a moderately incised channel (20-40 m) across a relatively smooth and extensive alluvial plain. The eastern termination of the alluvial plain was evidently between McKenzie Table and Squaw Leap/Kennedy Table, since the trachyandesite of both of the latter remnants rests directly on tonalitic bedrock. There is no indication that the Miocene river at the paleomeanders was confined in a bedrock canyon. Perkins West Table is thinner than the other flow remnants (\sim 35 m), and, while its northeastern edge is underlain by fluvial gravel, its western portions rest directly on tonalite, as does the nearby remnant at Pincushion Mountain (Fig. 4), suggesting that exposed bedrock formed a relatively planar pediment on the same grade as the alluvial fill. The lava flowing down the river channel evidently rose high enough in some places to spread out over the surrounding plain in a sheet a few kilometers wide (see CM, PM on Fig. 4). The preserved flow areas that are not channel remnants seem mostly to have been broad tributary valleys that were somewhat shallower than the main channel. The greater thickness of the flow filling the main channel and tributaries has enabled them to escape erosion over the past 9.3 m.y., while the thinner portions have largely been eroded.

Kennedy Table

This large table consists of an elongate plateau and narrow flat-topped ridges (Figs. 4 and 5); its scraggly outcrop pattern suggests that the lava had backfilled lateral tributaries, consistent with NNW increase in basal elevations by \sim 95 m (Fig. 4). Including its northern outliers, Kennedy Table is 8.8 km long, with its axis trending grossly \sim 160°. The base of the lava declines from \sim 730 m in the north to \sim 635 m at the south tip, reflecting an average slope of 10.8 m/

km (\sim 0.62° SSE), at a 60° angle to the 220° tilt azimuth. Across the narrow table, however, the southwest component of slope is hard to quantify with confidence and is variably estimated at 0.8–1.2° WSW. Preserved thicknesses range from 35 to 50 m. The roughly tabular but eroded surface of Kennedy Table has 5–10 m of local relief.

Bug Table

This is an 800-m-wide, V-shaped outlying remnant just northeast of Kennedy Table (Fig. 4). As the highest exposure among downstream remnants, the mildly eroded surface of Bug Table reaches an elevation >793 m at its east end and slopes $1.5-3^{\circ}$ WNW and SW along its arms. In addition to the slight westward inclination, the eroded surface has $\sim 5-10$ m of irregular local relief.

The base of the lava is at \sim 742 m at the foot of its northwest scarp and \sim 732 m along its southeast scarp. Thickness of the flow thus appears to increase from \sim 50 m to 60 m, roughly southward.

Squaw Leap

This is a narrow southwest-trending, flattopped ridge, 1.9 km long and only 100-400 m wide, which is the upstream-most remnant on the left bank, southeast of the modern river and 2.5 km southeast of the south tip of Kennedy Table (Fig. 4). A 2.5-km-long adjacent chain of seven small knoll-capping remnants (Fig. 4) may represent lateral filling of a Miocene tributary as their basal elevations climb ~25 m southeastward. From the NW remnants of Kennedy Table to the SE end of the chain near Squaw Leap, the lateral distance is 13 km (Fig. 4), indicating lowland spreading of the lava flow when it emerged from whatever had been its upland valley course. The base of the Squaw Leap table descends ~46 m southwestward, at a slope of 1.38°, the steepest basal value observed among the remnants. There is 10-15 m of local relief on the eroded table top. Preserved thickness of the lava flow increases from only \sim 35 m at the northeast end to \sim 50 m on the southwest cliff.

Between Squaw Leap and McKenzie Table, the next remnant southwest, the gap between their bases represents a descent of $\sim \! 100$ m in 3.25 km for a slope of 1.77°. As the azimuth connecting the tips of these remnants is 232°, correction of the apparent dip to an azimuth of 220° yields a slope of 1.81°, which is considerably steeper than the bases of the remnants preserved.

McKenzie Table

This narrow sickle-shaped table is 5.4 km long, and its width ranges from 800 m to as

little as 200 m, but there is also a contiguous northeast salient that forms a kilometer-wide plateau that forks eastward into a pair of branches (Fig. 4). Much of the table is in the Ruth McKenzie Table Mountain Preserve now administered by the Sierra Foothill Conservancy. Its eroded surface slopes from 620 m on the northeast plateau to 530 m at the southwest rim, representing a slope of 25.4 m/km or 1.45° along a dip azimuth of 220°. However, on the same line, the base of the lava descends only \sim 79 m, yielding a gradient of \sim 19 m/km or only 1.1°. As noted by Huber, this reach has a gentler basal gradient than other table remnants upstream or downstream. Estimated thickness of the lava ranges 55-67 m.

The north end of McKenzie Table is only 1.3 km east of the modern river (Fig. 5), and the base of the lava there is now \sim 385 m higher than the reservoir-drowned thalweg. Fluvial gravel directly under McKenzie Table is exposed on many sides. Capped by baked soil, gravel visited below the southeast scarp is 41-57 m thick and rests on an irregular tonalite surface. All trachyandesite remnants downstream of McKenzie Table likewise rest on gravels, but none of those upstream of it is known to expose any Miocene river sediments. Cretaceous tonalitic bedrock is exposed beneath all the lava-flow remnants farther upstream and beneath the intervening gravels from McKenzie Table downstream.

Table Mountain

Just southwest of McKenzie Table, this is another narrow, arcuate, flat-topped ridge, 4.5 km long and 350–700 m wide, which forks into two slender ridges at its southwest end (Fig. 4). Preserved thickness of the lava here ranges from 45 to >60 m. From north to south, its eroded surface descends from $\sim\!530$ m to 450 m, and its base goes from $\sim\!485$ m to $\sim\!395$ m, both yielding gradients of $\sim\!24$ m/km or 1.4° SW. Although the gross outcrop of the table trends SSW, its northern surface actually slopes $\sim\!2^\circ$ SW, and the surface of its southwest arm slopes $\sim\!1.45^\circ$ SW (or 1.5° corrected to 220°). Fluvial gravels crop out widely at its base.

Perkins West Table

The westernmost table preserved, this low-relief remnant lies just south of the Big Bend meander of the drowned modern river (Figs. 4 and 5). Although not as arcuate as its neighboring remnants, its northern margin is conspicuously concave toward the river and underlain there by fluvial gravels. The table extends

1.6 km east-west and 700 m north-south, and it has a narrow NNE panhandle. Thickness observed along its scarps ranges 30–40 m, thinner than most remnants upstream. Its roughly planar but eroded surface has 10–15 m of local relief. From northeast to southwest, the base of the lava drops \sim 48 m in 2.2 km, yielding a basal gradient of 22.2 m/km or 1.27° (corrected to 1.29° at 220°).

Little Dry Creek

A 3.5-km-long chain of nine remnants of the lava flow caps the ridge forming the north wall of Little Dry Creek, 5-7 km south of Friant Dam (Fig. 4) and \sim 4.4 km southwest of the nearest large remnant (Perkins West Table). The chain is the most distal segment of the trachyandesite lava preserved, and its trend at 230°-235° is a bit more westerly than the gross trend of the large remnants upstream (210°-220°). The largest of the nine lava-capped knolls along the chain is only 500 m long; several are 100-250 m across (normal to the flow direction), and some are smaller (Fig. 4). All are eroded, they range in thickness only from 5 to 25 m, and none preserves a planar table top. The chain rests directly on ~46 m of fluvial sand and gravel deposits, which in turn rest on Cretaceous tonalite. The smooth contact atop the gravels declines southwestward in elevation from \sim 287 m to 207 m, a present-day gradient of 23.5 m/km or 1.346° (corrected to 1.367° at 220°). The gap between the Little Dry Creek chain and nearest large remnant at Table Mountain, which likewise rests on the gravels, represents a gradient of ~25.5 m/km (110 m/4.32 km) or 1.46°.

As a well-preserved linear segment of the late Miocene riverbed, the trachyandesite-gravel contact at Little Dry Creek may be the most planar and thus the most reliable basal slope marker beneath the many lava-flow remnants. Because it is located at the floodplain transition to the Central Valley, and because thick sheets of fluvially transported sandy-silty ash are interbedded with the gravels (as described below), the distal lava-flow section at Little Dry Creek may likewise have had the gentlest and smoothest original depositional gradient anywhere preserved.

Inferences from Basal Contours

Contour lines drawn on Figure 4 connect points of equal elevation on the base of several remnants of the lava flow. Taken altogether, the contours roughly define a basal slope azimuth at 210°, whereas the bases of the Little Dry Creek remnants define a slope azimuth at 230°–235°.

The steepest basal gradient recognized is 1.38° SW beneath Squaw Leap, and the gentlest is 1.1° SW beneath McKenzie Table. The average gradient beneath the combined meandering segments of Table Mountain and McKenzie Table is 1.18° SW, and that from Bug Table to the southwest scarp of Kennedy Table is 1.19° SW. As mentioned above, however, gaps between tables (Fig. 4) have slopes of 1.46° (Table Mountain-Little Dry Creek) and 1.81° (Squaw Leap-McKenzie Table). The average basal gradient embraced by all contour lines in Figure 4 is 1.26° SW or, for only those on the modern left bank (Squaw Leap to Table Mountain), 1.38° SW. The nine Little Dry Creek remnants define a smooth basal gradient of $\sim 1.367^{\circ}$ SW, and the average gradient from the SW end of Squaw Leap to distal Little Dry Creek is 1.34° SW. The inconsistency of basal slopes beneath the several remnants leads us to favor the one beneath the Little Dry Creek distal floodplain remnants as the most reliable present-day surface for calculating the amount of rigid block tilt since the late Miocene.

For comparison, the linearized gradient of the modern river (neglecting its meanders) is 0.53° SW (195 m in 21 km) from Kerckhoff Dam to Friant Dam (Fig. 4). The distal reach just above Friant Dam, however, has a gradient of only 0.075° W (6 m in 4.6 km). Below Friant Dam, where the river enters the Central Valley and topographic maps have a 5 ft (1.5 m) contour interval, the gradient diminishes to 0.03°–0.01°. As a primary gradient for the most distal parts of the lava flow, Huber (1981) postulated a Miocene floodplain gradient of 1 m/km (0.057°), a value we find plausible (or perhaps even slightly excessive).

Inferences about the Location of the Miocene Thalweg

Kennedy Table and Squaw Leap face each other across a 2.5 km erosional gap occupied by the modern river. The bases of both reflect the general SW slope illustrated by the contour lines in Figure 4, but the outcrops preserved also show components of slope toward each other. Along the 8.8 km length of the narrow Kennedy Table remnant, its basal elevation drops ∼95 m toward the SSE. Squaw Leap and its SE chain of remnants define a modest basal slope that drops \sim 25 m to the NW (Fig. 4). The facing cliffs of the two remnants are 45-50 m thick. It thus appears plausible that the Miocene thalweg and axis of the lava flow lay between them and that the sets of remnants to the SE and NNW represent lateral spreading of the lava upon entering a broad low-relief plain. To the north, we observed no local thickening of the lava at Bug

or Kennedy Tables to suggest that the Miocene paleothalweg had passed beneath them.

McKenzie Table and Table Mountain together define a meandering lava ridge 11 km long (Fig. 4). Huber (1981) argued that the meanders formed by subsequent erosion of a ponded lava flow, rather than by the flow filling a meandering channel. Above, however, we argue in favor of the previous view that these meanders do reflect the Miocene river channel. Taken together, McKenzie Table and Table Mountain define an average basal gradient of 1.18° along a dip azimuth of 220°, gentler than beneath and between other remnants. The base of Squaw Leap is steeper with a true dip (at 220°) of 1.38°, and that of Kennedy Table is gentler but variable; both, however, have significant NW and SE components of inward slope toward the inferred channel axis, as discussed above. Moreover, Squaw Leap, Kennedy Table, Bug Table, and their satellites reveal no basal gravels, whereas all remnants from McKenzie Table downstream to Little Dry Creek overlie thick fluvial gravels. Furthermore, a paleothalweg that continued from Table Mountain to the Little Dry Creek remnants would have trended 220°, whereas a Miocene course north of Perkins West Table would be an unlikely route to Little Dry Creek (Fig. 4).

Crook Mountain and Pincushion Mountain (Fig. 4) are capped by small remnants of the lava flow (each resting on bedrock \sim 3 km NW of the meandering McKenzie Table-Table Mountain segments) that add useful perspectives on the original extent of the Miocene lava apron. The 30-m-thick remnant banked against the summit of Crook Mountain has its base at \sim 1900 ft (579 m), 55 m lower than the nearest part of Kennedy Table but 43 m higher than the NW base of McKenzie Table, which lies 2.9 km SE. The base of the 30-m-thick remnant (of two flows) atop Pincushion Mountain is at \sim 1480 ft (451 m), similar in elevation to the NW end of Table Mountain, 3 km SE. Accordingly, we infer that the lava remnant at Crook Mountain was well upslope from the floor of the river channel but the lava at Pincushion Mountain was not.

LATE MIOCENE FLUVIAL SEDIMENTS BENEATH THE TRACHYANDESITE

A 46 m section of fluvial gravels beneath the lava flow north of Little Dry Creek was logged by Janda (1966) and revisited by us in 2019. The section consists of well-rounded, cobblebearing, pebble-dominant alluvium with an arkosic sandy matrix that alternates with fluvial beds of white rhyolitic sand-silt (marked by X in Fig. 4). As at McKenzie Table, where the gravels are 41–57 m thick, most clasts are metamorphic

rocks, granitoids are sparse, and volcanics are absent other than ash and rare pumice granules. At Little Dry Creek, the lower 23 m of the 46-mthick sedimentary section contain three horizontal layers of weakly indurated, case-hardened, tuffaceous sand, well exposed on vertical faces. The uppermost of the three is 2 m thick, lithicfree, locally laminated, and poor in crystals. Its lowest 1 m contains a scattering of indurated ash pellets 3-12 mm across, which weather out in its tan-gray case-hardened crust. The middle layer is 2-3 m thick and similar but massive and lacks pellets. The lowest layer, 2-3 m thick, is almost pure white rhyolitic ash, marked by high-energy cross-bedding in its basal \sim 1 m but massive above. It is fines-poor, dominantly sand-sized, and almost devoid of lithics and crystals, and it carries sparse crystal-poor pumice, which is mostly <5 mm but as big as 15 mm. Deposited directly on coarse gravels, the lowest layer thus appears to be a virtually uncontaminated deposit of vitric ash from a large eruption >150 km upstream that briefly flooded the river and lost its crystals and lithics during fluvial transport downstream. The higher ash layers consist dominantly of the same ash but are mixed with a little nonvolcanic sand. All three were deposited on a low-relief floodplain.

The pumice has suffered hydration and Na loss (7.1% loss on ignition [LOI]; 2.62 wt% Na₂O) but (recalculated to 100% volatile-free basis) is unequivocally rhyolitic (72.5% SiO₂; 0.2% TiO₂, 5.3% K₂O; 0.03 wt% P₂O₅; 228 ppm Rb). The primary eruptive deposit has not yet been proven, but candidates include two late Miocene rhyolitic ignimbrites north of Long Valley, one of which gave a sanidine K-Ar age of 11.7 \pm 0.1 Ma (Huber, 1981; unit Trac of Hildreth and Fierstein, 2016).

A different pumice, trachydacitic (latitic) in composition (\sim 64% SiO₂; 5.1% K₂O), was reported by Huber (1981) on the opposite (north) side of the same ridge north of Little Dry Creek (Fig. 4), where a discrete layer rich in pumice pebbles is interbedded in the gravels. Huber obtained a plagioclase K-Ar age of 11.3 \pm 0.3 Ma for the pumice and plausibly correlated it with the "latite ignimbrite" of Gilbert et al. (1968), which is of similar age, mineralogy, and composition and crops out widely in eastern Mono Basin and the Adobe Hills. No other compositionally and chronologically comparable eruptive unit is known in or near the San Joaquin drainage system. The presence of the two types of pumice clasts at Little Dry Creek confirms that the Miocene San Joaquin River headed east of the modern Sierran divide in what later became Mono Basin, prior to blockage of its course by Pliocene basalts and tectonic beheading by early Quaternary range-front faulting.

COMPOSITION AND AGE OF THE TRACHYANDESITE

The trachyandesite is the product of a single continuous eruption. At a few distal sites, a pair of 15–25-m-thick flow units each has a basal columnar zone, but the duality is seen only at McKenzie Table, Perkins West Table, and Pincushion Mountain. As an atypical feature, it may represent distal slowing, budding, and local self-overriding of the flow. Elsewhere, well-exposed cliffs along the many remnants, some 30–70 m high, reveal only a single lava flow.

The chemical composition is strikingly uniform for an eruptive unit at least 90 km long. Table 1 gives data for 11 samples, representing the vent complex and the downstream tables and exhibiting ranges of only 57.96%–58.19% SiO₂, 1.05%–1.08% TiO₂, 0.46%–0.52% P₂O₅, 12–14 ppm Sc, 147–153 ppm V, 88–94 ppm Ce, 952–977 ppm Sr, 258–272 ppm Zr, 21–23 ppm Y, and 18–19 ppm Th.

Thin sections have 15%–20% plagioclase, ~1% clinopyroxene, <1% olivine, and trace opaque oxide minerals in a groundmass rich in microlites and commonly still partly glassy. Most feldspars are lath-shaped, 0.5–3 mm long, and strikingly twinned; a minority of feldspars are sieve-textured. Clinopyroxene and olivine are mostly microphenocrysts (0.1–0.5 mm), but rare crystals of each reach 1–2 mm. The Fe-Ti oxides are predominantly 0.1–0.3 mm across, but rare crystals reach 0.5 mm. Sparse quartz xenocrysts are present. The only difference noted between vent and downstream samples is a greater tendency for olivine to be altered to iddingsite in the latter.

We previously published analytically indistinguishable 40 Ar/ 39 Ar ages for the vent complex and for Perkins West Table; analytical data are in table 2 of Hildreth and Fierstein (2016). Material dated was a plagioclase separate for the vent and devitrified groundmass for the downstream lava. Subsequently, the Menlo Park geochronology laboratory updated its laboratory standards to align better with other laboratories (Fleck et al., 2019), rendering the ages slightly older. The reported ages were 9164 \pm 17 ka and 9192 \pm 15 ka, and they are here recalculated to 9321 \pm 17 and 9349 \pm 15 ka (weighted mean 9337 \pm 11 ka).

POST–9.3 Ma TILT OF THE SIERRA NEVADA BLOCK

Gradient Reconstruction for Table Mountain/McKenzie Table Meanders

The tilt analysis of Huber (1981) depended critically on the assumption that the gradient of

the Miocene San Joaquin River at the tables had been similar to adjacent reaches of the modern river. This assumption has been criticized on the basis that "only qualitative observations were used to justify assigning the modern river's gradient to its 10 Ma bed" (Gabet, 2014, p. 1236). Fortunately, the preservation of large paleomeanders of the Miocene river offers the opportunity to quantitatively evaluate the depositional river gradient. For modern river meanders, including those of the San Joaquin River, there is generally no dependence of gradient on flow direction (Wakabayashi, 2013). Lindgren (1911) pointed out that, if a belt of meanders were tilted, sections of meanders that were oriented perpendicular to the axis of tilting of a mountain range would be most strongly tilted, while those parallel to the axis of tilting would undergo no tilting. Jones et al. (2004) and Wakabayashi (2013) quantified this observation by showing that the variation of meander gradient produced by tilting depended on the cosine of the azimuth of each portion of the meander relative to the direction of tilt (i.e., perpendicular to the axis of tilting). Thus, a cosine dependence of the paleochannel gradient constitutes a quantitative demonstration of tilting, and the original gradient can be reconstructed by subtracting an amount of tilt that returns the gradients to a uniform value.

Some applications of this principle in the Sierra Nevada have been criticized on the grounds that discontinuous sections of paleochannel must be connected, and these sections may not have actually been contemporaneous, or they may have been offset by faulting (Gabet, 2014). Table Mountain and McKenzie Table (TM and MT in Fig. 4) are not subject to these criticisms because they are nearly continuous (one break in the middle) and can be demonstrated to compositionally be a single lava flow and, since the meanders were preserved due to infill by a single lava flow, can be confidently dated to one geological instant.

The type of analysis described above is based on fitting of cosine curves to the gradient data, and this requires a significant number of data points to be statistically significant. Ideally, we would use data from the base of the lava flows for this purpose, since these points presumably preserve the original channel elevation. We have done this for the gradient reconstructions described above, which employed a small number of widely spaced observations. However, the number of points at which the basal contact is exposed under Table Mountain and McKenzie Table is small, due to cover by talus and colluvium from the sides of the eroding flows. For this analysis, therefore, we were forced to use data points on the surfaces of the flows. Since the flows are of relatively constant thickness (Huber, 1981), and the channels they occupied were apparently meandering across an alluvial plain with few or no constrictions (see discussion above), we assume that the gradients of the flow surfaces reflect the underlying channel gradients.

As we cited above, an alternative interpretation was proposed by Huber (1981), who speculated that the apparent meanders were merely fortuitous remnants of a ponded lava flow that occupied a broad valley. In this case, after tilting, a fortuitous meandering path down the planar flow would also produce a cosine dependence of gradient on azimuth, even though the gradient was independent of any actual channel. Above, we have presented geological arguments against Huber's planar-flow hypothesis, but we also point out that the azimuth/gradient data permit an internal test of this hypothesis. If the data set reflects a meandering channel gradient, then when any imposed tilt is removed, the azimuthindependent residual gradient value should be reasonable for a meandering river, including data points that are from azimuths perpendicular to the regional slope. However, any path segment on a horizontal or inclined plane (e.g., a planar lava flow) that is perpendicular to the regional slope, in this case, the gradient of the planar flow, will have a zero gradient (i.e., "following the contour"). Thus, when tilt-corrected, the measured gradients will converge to a gradientindependent value of zero.

The alternative outcomes can be summarized as follows. If the Table Mountain and McKenzie Table flows are fills in a meandering river channel of relatively constant cross section, then the measured gradients should have a cosine dependence on azimuth relative to the regional slope, and, when the imposed tilt is removed, they should show minimal deviation from a constant gradient at a value that is positive (i.e., downhill) and reasonable for a meandering river. If the flows descended a river channel, but some factors (e.g., variable cross section or changing flow viscosity) caused the flow surface gradient to deviate significantly from that of the underlying channel, the data would not be expected to exhibit a cosine dependence on azimuth, but rather to show some systematic deviation from cosine form. No amount of tilt removal would produce a constant gradient with azimuth. Finally, if the data points are from a fortuitously preserved path down a planar flow surface, they will exhibit cosine dependence on azimuth, but the cosine curve will be flattened to an azimuthindependent value only when the full contemporary regional slope is subtracted, and the residual value will be zero, which is not reasonable for any real river.

In order to fully characterize the surface, we obtained Universal Transverse Mercator (UTM)

coordinates and elevations for the centerlines of the two tables using the USGS NED1 30 m digital elevation model, following the leasteroded portions of the mesa tops (Fig. 6A). In total, 767 data points were taken (Supplemental Material¹). The data from the ends of the mesas. which were eroded, and any other obviously eroded points were removed. The north-facing ends of the flow, truncated by erosion of the San Joaquin River canyon, are transversely fractured due to progressive slumping into the canyon and were excluded. The flow surface itself, however, has obviously been at least somewhat eroded in many places during 9.3 m.y. of exposure. Inasmuch as the elevation gradient is the first derivative of the topographic profile, it is quite sensitive to erosion. We therefore fitted the topographic profile data with polynomial functions (Fig. 6A) and resampled every 10th point (~100 m spacing) to recover the kilometer-scale gradient of the flow (see Supplemental Material). The gradient as a function of meander azimuth is shown in Figure 6B. The uncertainty bars on the data points (0.15°) represent one standard deviation of the differences between the cosine curve and the data.

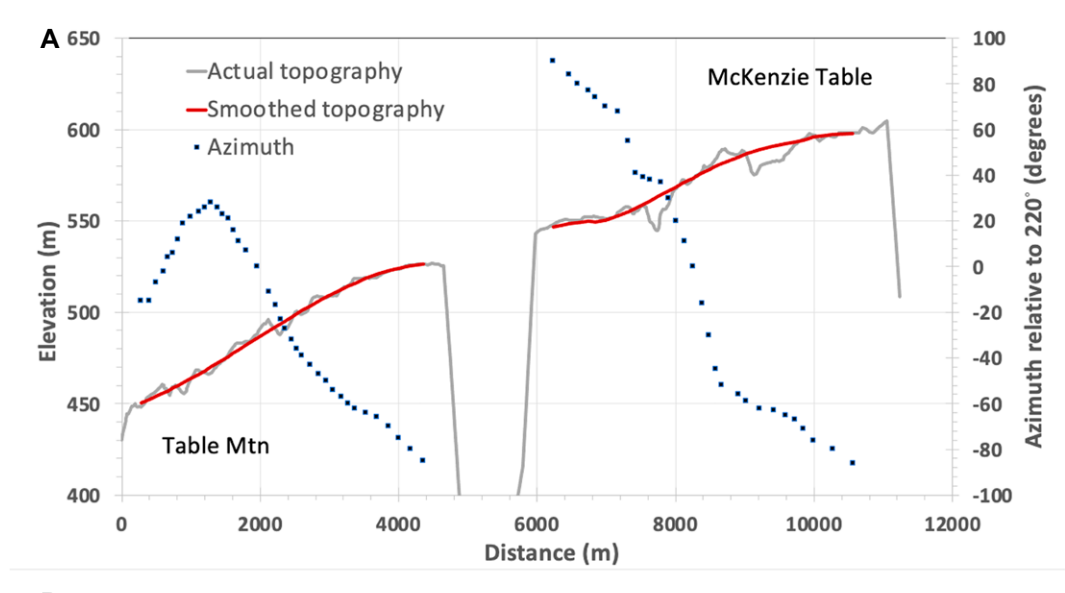
The azimuthal dependence of dip can be fitted well with a cosine function having a maximum of 1.30° at 220° azimuth, demonstrating that the flow has been tilted downward toward 220°. The amount of tilt was identified by subtracting the cosine-dependent tilt from each data point for a large range of tilt values. Removing the actual amount of tilt should yield an azimuthindependent array of data points, for which the mean value represents the depositional gradient. The chi-squared function was computed from the difference between each tilt-corrected gradient point and the mean of all the tilt-corrected gradient values for each tilt value tested. The tilt producing the minimum sum of chi-squared values was selected as the optimal tilt value (Fig. 6B). Subtraction of 1.07° of dip restored the data to an azimuth-independent configuration (Fig. 6B), indicating total tilting since 9.3 Ma of $1.07^{\circ} \pm 0.06^{\circ}$. The average inclination calculated for the minimum chi-squared value was $0.23^{\circ} \pm 0.05^{\circ}$, which corresponds to the depositional gradient of the paleochannel. The reduced chi-squared value for 1.07° of tilt was 1.02; assuming 0° of tilt increased the reduced chi-squared value to 5.66.

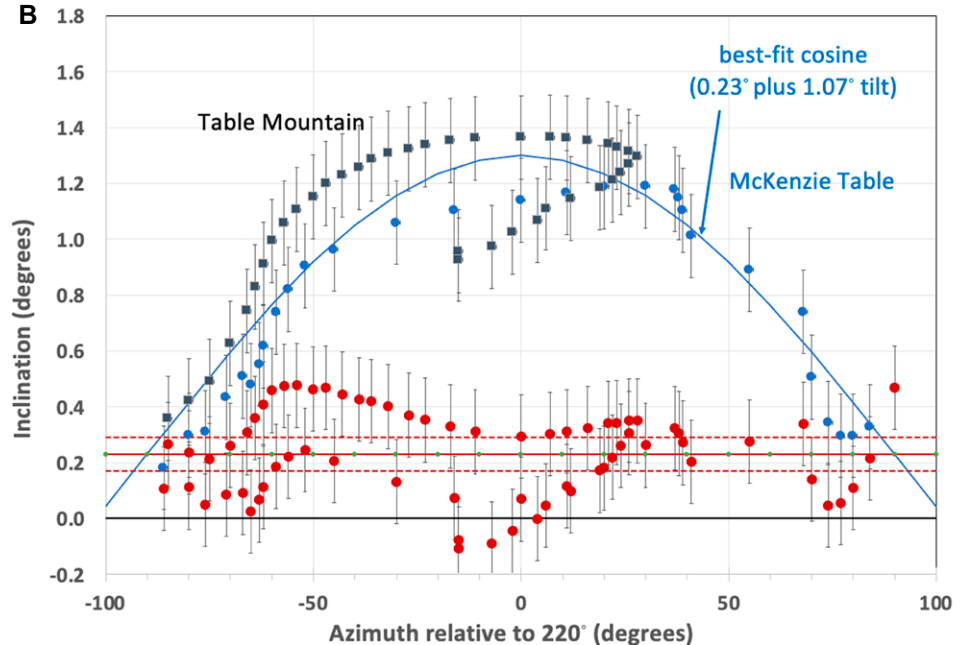
In Figure 6C, we compared the reconstructed paleogradient of the Miocene San Joaquin River with modern channel gradient data obtained from short segments of meanders over a fairly long reach of the river by Wakabayashi (2013). The modern average gradient from his data set is $0.33^{\circ} \pm 0.22^{\circ}$, compared with the paleogradient of $0.23^{\circ} \pm 0.05^{\circ}$. We performed a more local measurement of the modern river gradient, extending along the path of six meanders opposite the Miocene flow remnants (from just above to just below Millerton Lake), which yielded a value of 0.18°. Following Huber, we note that, like the paleomeander analysis, the values quoted above represent the inferred gradient of the channel itself, which must be less than that of the linear landscape gradient over many meanders. To obtain the large-scale linear gradient of the river, the channel gradients must be multiplied by the sinuosity of the channel, which we measured to be 2.0 here. Applying the same correction to the inferred Miocene channel gave a linear, landscape-scale value of $0.46^{\circ} \pm 0.05^{\circ}$.

Our quantitatively reconstructed value for the Miocene San Joaquin River gradient is somewhat larger than Huber's value (1981, p. 13), which he described as "possibly as low as" 0.06°; however, this was based on measurements performed west of Friant Dam, considerably downstream of the McKenzie Table/Table Mountain paleomeanders. Our magnitude of tilting (1.07°) is therefore a little less than that inferred by Huber: 1.22°. Unlike Huber's analysis, our tilting value was derived directly from the meander data and does not depend on any external assumptions regarding the gradient during the Miocene.

The data presented in Figure 6 enable evaluation of the alternative possible outcomes described above. First, the uncorrected data do exhibit a clear cosine dependence on azimuth. This indicates that the surface traced was either a lava flow of relatively constant thickness following a channel, or it was an inclined plane, but it was probably not from a lava flow that varied significantly in thickness and thus deviated from the channel gradient. Second, when chi-squared minimization was used to identify the optimal tilt, the residual (presumably depositional) tilt was $\sim 0.23^{\circ}$, and this is clearly greater than zero. This is consistent with the geological evidence in indicating that the lava flow followed an alluvial channel rather than forming a broad, inclined sheet. Finally, the optimal inferred value for the depositional tilt is very close to that of the nearby, meandering, modern San Joaquin River. It is thus eminently reasonable as a value for the depositional grade of the ancestral San Joaquin River and, in combination with other geological evidence described above, supports the inference

¹Supplemental Material. Table S1: Data for full topographic profile up Table Mountain and McKenzie Table Sections highlighted in red show significant erosion; Methodology for Meander-Tilt Analysis. Please visit https://doi.org/10.1130/GSAB.S.14885451 to access the supplemental material, and contact editing@geosociety.org with any questions.





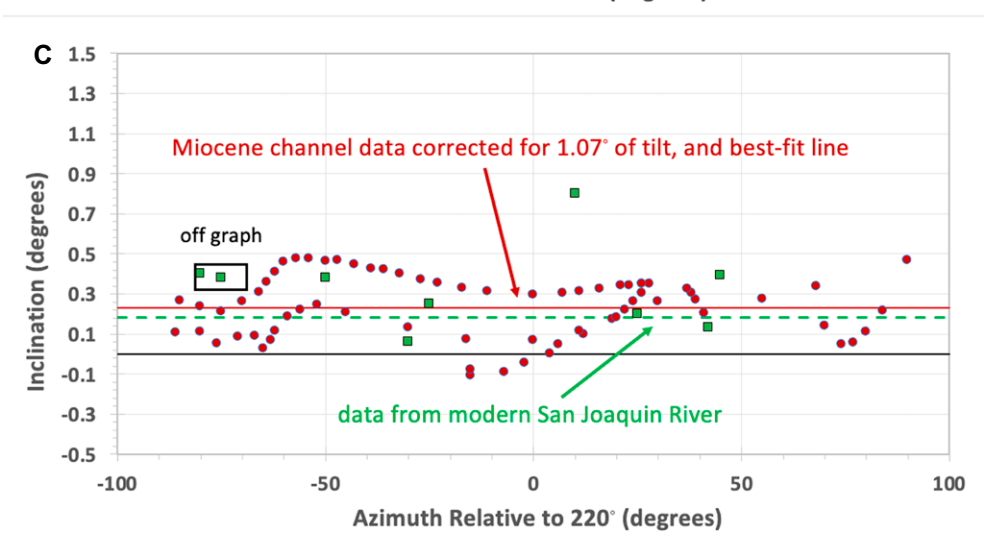


Figure 6. (A) Topographic profile up centerline of Table Mountain and McKenzie Table (TM and MT in Fig. 4), starting from Universal Transverse Mercator (UTM) Zone 11S, E 266686, N 4096832. Smoothed profiles of topography and azimuth used in the mathematical analysis are also shown. (B) Measured, smoothed, flow-top gradient as a function of azimuth relative to tilt direction (220°), with best-fit cosine function, and same data corrected for 1.07° tilt toward 220° . (C) Fossil meander gradient data corrected for 1.07° of tilt compared to similar gradient data for the modern San Joaquin River from Wakabayashi (2013) and from this paper.

that McKenzie Table and Table Mountain are preserved meanders.

Range-Scale Tilt Analysis

Figure 7 illustrates a line joining the most distal outcrop at Little Dry Creek (basal elevation 207 m) with the vent intrusion—lava flow transition (at 2760 m). The line trends 220°, which is (not coincidentally) the tilt azimuth first estimated by Huber (1981); it represents a horizontal distance of 89 km, and it thus defines a present-day average basal gradient for the lava flow of 1.643°. The line is for reference only, and it is not a profile, as the concave profile of the San

Joaquin River would be well below it, as verified by the projections of basal gradients recorded at the various downstream remnants.

The diagram shows modern average basal gradients (all adjusted to 220°) observed for the Little Dry Creek chain (1.367°), the combined Table Mountain–McKenzie Table sinuous reach (1.18°), and Squaw Leap (1.38°). Also shown are Miocene river gradients at the time of emplacement of the lava flow (9.3 Ma), as estimated by Huber (1981) for the distal floodplain beneath the Little Dry Creek remnants (<0.057°) and for the short reach near Squaw Leap (0.33°).

The Miocene gradient of 0.46° shown in Figure 7 for the sinuous McKenzie Table–Table

Mountain reach (Fig. 4) is from the meanderrestoration analysis described above. The sum of the original gradient plus the added tilt (1.07°) is similar to the modern basal gradient observed for the Little Dry Creek chain (1.367°) and for the whole left-bank set of remnants (1.38°)—Squaw Leap to Little Dry Creek—all values adjusted to the 220° tilt azimuth.

Subtracting those Miocene gradient estimates from the observed 1.643° gradient yields vent uplifts of 2464 m (for an original dip of 0.057° from Huber), 1835 m (for 0.46° from the meander-tilt analysis), and 2040 m (for 0.33° from the Squaw Leap reach). The gentle Miocene floodplain gradient assumed by Huber (0.057°)

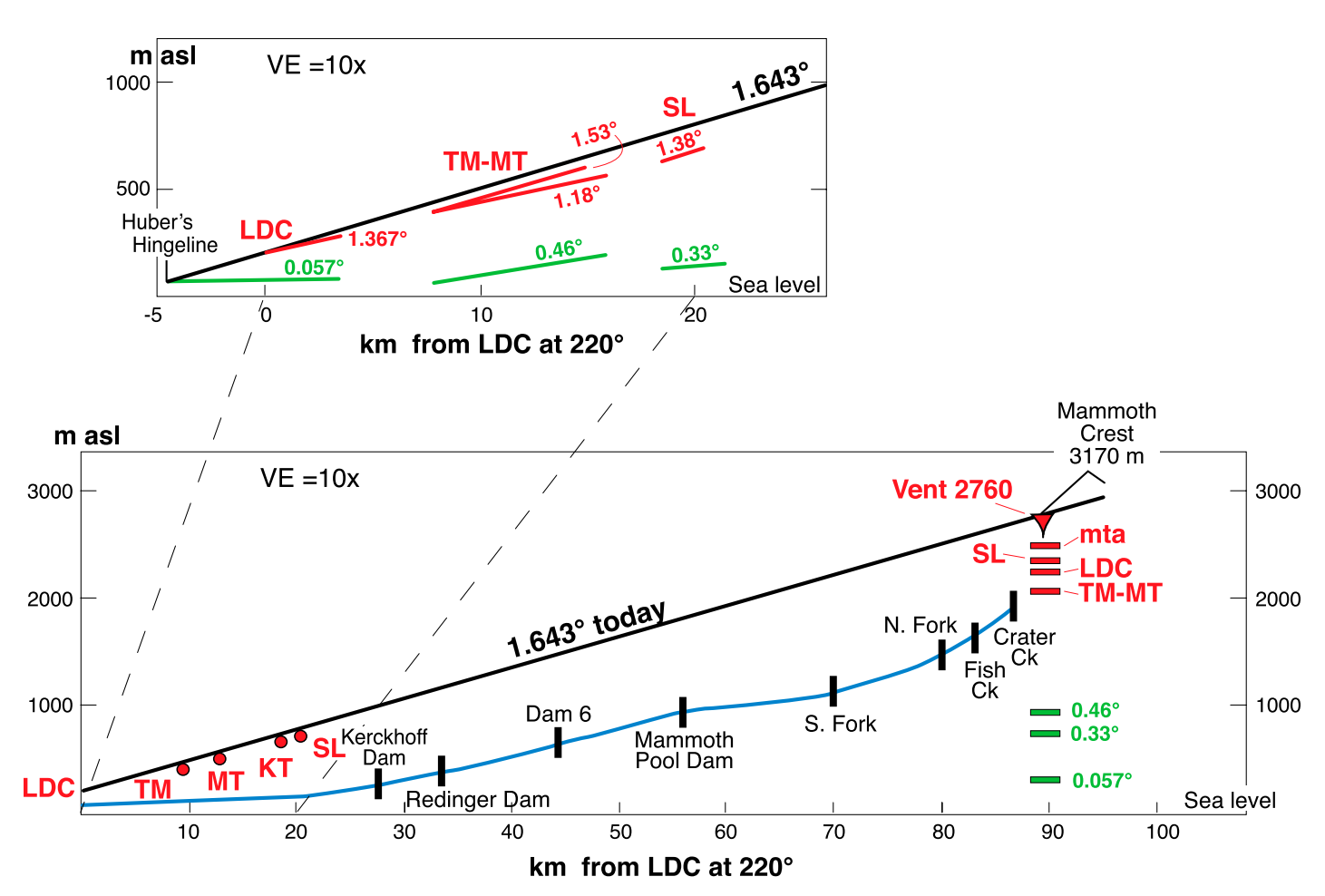


Figure 7. Longitudinal profiles of San Joaquin River projected onto a vertical plane that strikes N40°E, thus embracing a Sierran tilt azimuth of 220°. Axes are in kilometers northeast of distal lava remnant at Little Dry Creek (LDC) and in meters above sea level. Smaller panel expands scale for downstream remnants. Both panels have 10× vertical exaggeration (VE). Linear horizontal distance from vent complex to Little Dry Creek is 89 km. Line joining bases of lava flow at Little Dry Creek and at vent now dips 1.643°; it is a limiting line only, with no relation to any Miocene stream profile, which necessarily was concave and lay below this line. Modern basal dips are shown as red lines on smaller panel for lava-flow remnants: Squaw Leap (1.38°, SL), meandering Table Mountain–McKenzie Table (1.18°, TM–MT), and Little Dry Creek chain (1.367°, LDC). Green lines indicate Huber's estimates of Miocene gradients at Little Dry Creek and Squaw Leap. Green line 0.46° and red line 1.53° are from the meander-tilt analysis (mta). On larger panel, red lines indicate elevations where the measured basal planes project relative to vent complex 89 km NE. Likewise, green lines in small panel show where estimated Miocene gradients project 89 km NE (green bars on larger panel). Hinge line of rigid-block tilt postulated by Huber (1981) is 4.5 km west of Little Dry Creek. Projected river profile (blue line) is that of trunk stream today. Mammoth Crest is present-day Sierran crestal drainage divide along the 220° projection. Ck—Creek; KT—Kennedy Table.

certainly underestimates the average of the 89-km-long Miocene profile, which must have steepened upstream. Huber (1981) had estimated a present-day 1.28° gradient at Little Dry Creek (less than our observed 1.367°), from which he calculated 2150 m of uplift of the range crest (or 1864 m uplift of the now-identified vent). From the meander-tilt analysis, we have calculated a gradient of 1.53° (1.07° of tilt and 0.46° pretilt), from which 1880 m uplift was calculated for the crest (or 1660 m for the vent). Uncertainty and variability of modern gradient measurements and of paleogradient estimates are significant, but it nonetheless remains clear that ~ 2 km of rock uplift due to tilting has taken place since 9.3 Ma.

Figure 7 further shows that projection 4.86 km farther northeast of the trachyandesite vent to the Sierran divide falls 270 m short of the 3170 m Mammoth Crest, suggesting that range-crest topography had steepened sharply northeast of the Miocene vent, then as now.

Huber (1981) calculated crest uplift from tilting of the downstream flows assuming that this part of the Sierra Nevada has undergone post–9.3 Ma rigid-block tilt without perceptible warping or faulting. This was challenged by Gabet (2014) as "unlikely." Our weighing of the evidence supports rigid-block tilt. First, most longitudinal stream profiles worldwide are concave upward, as are nearly all modern

Sierra Nevada river profiles (e.g., Clark et al., 2005; Huber, 1990; Matthes, 1965). Therefore, the source vent for a lava flow in the headwaters being located below a projection of the downstream channel would constitute good evidence that the profile had been convexly warped. This is not the case for the vent of the Trachyandesite of Kennedy Table. Figure 7 shows elevations of projections to the vent of the basal gradients observed at Little Dry Creek, McKenzie Table—Table Mountain, and Squaw Leap. Because the vent is actually at higher elevation than the projections, relations are consistent with a typical concave-upward, upstream-steepening Miocene river gradient for the long profile between the

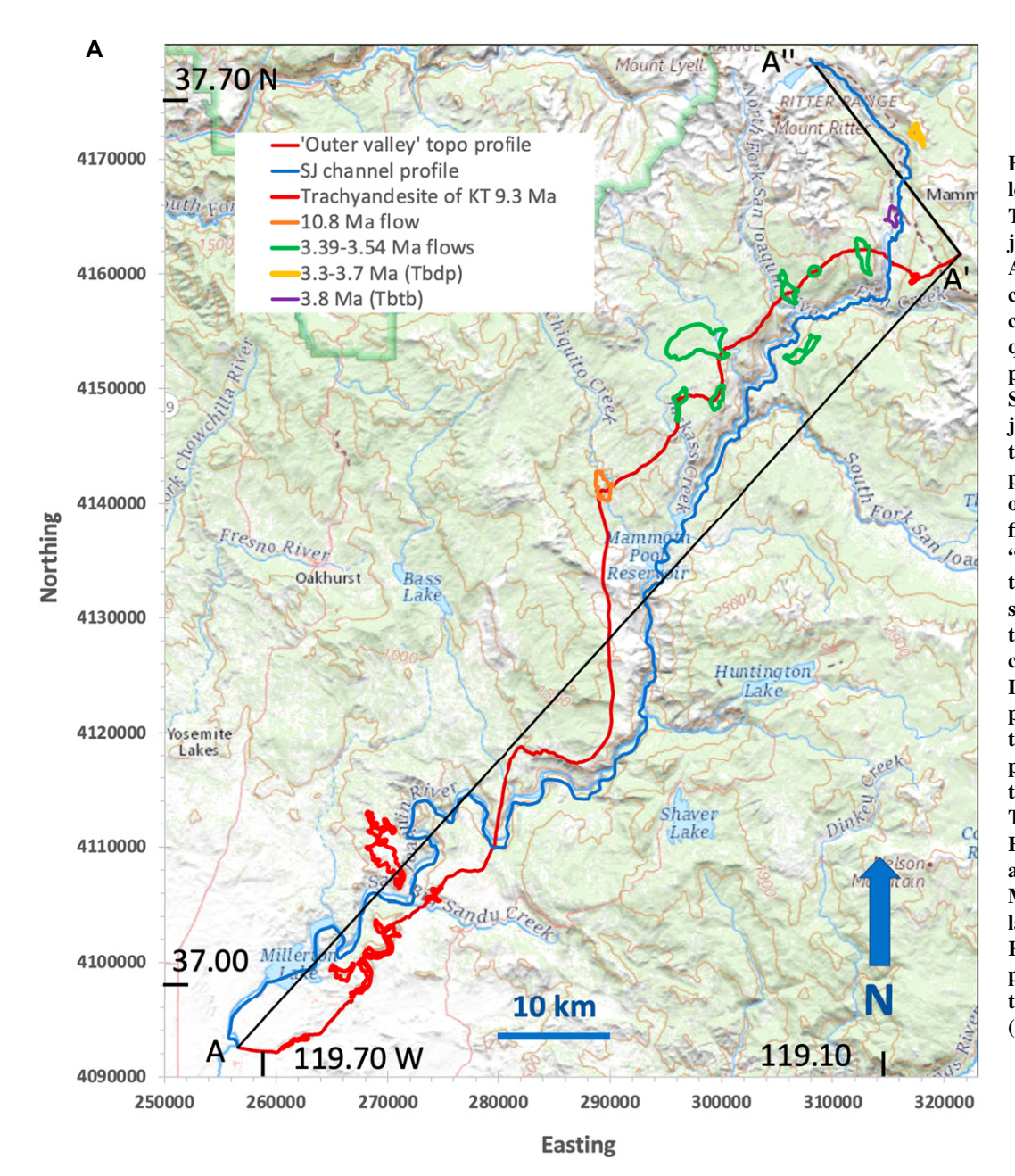


Figure 8. (A) Map showing location of cross section in B. Topographic profile was projected onto planes A-A' and A'-A". Lava flows shown on cross section are indicated by colored outlines. S.J-San Joaquin River. (B) Topographic profiles of the channel of the San Joaquin River and the adjoining "outer valley" of Matthes (1960). The "outer valley" profile is entirely projected onto A-A', but the channel profile switches to A'-A" where the "outer valley" profile crosses the San Joaquin River for the second time. "SJR" indicates the location where the profile crosses the San Joaquin River. Lava flows intersected by the profile are shown only where they intersect, but flows off the profile are projected in their entirety. Ages of the 10.8 Ma flow, Tbdp, and Tbtb flows are from Hildreth and Fierstein (2016) and U.S. Geological Survey Menlo Park Ar-geochronology laboratory work in progress. KT-Kennedy Table. Sawtooth pattern reflects hanging tributaries discussed by Matthes (1960).

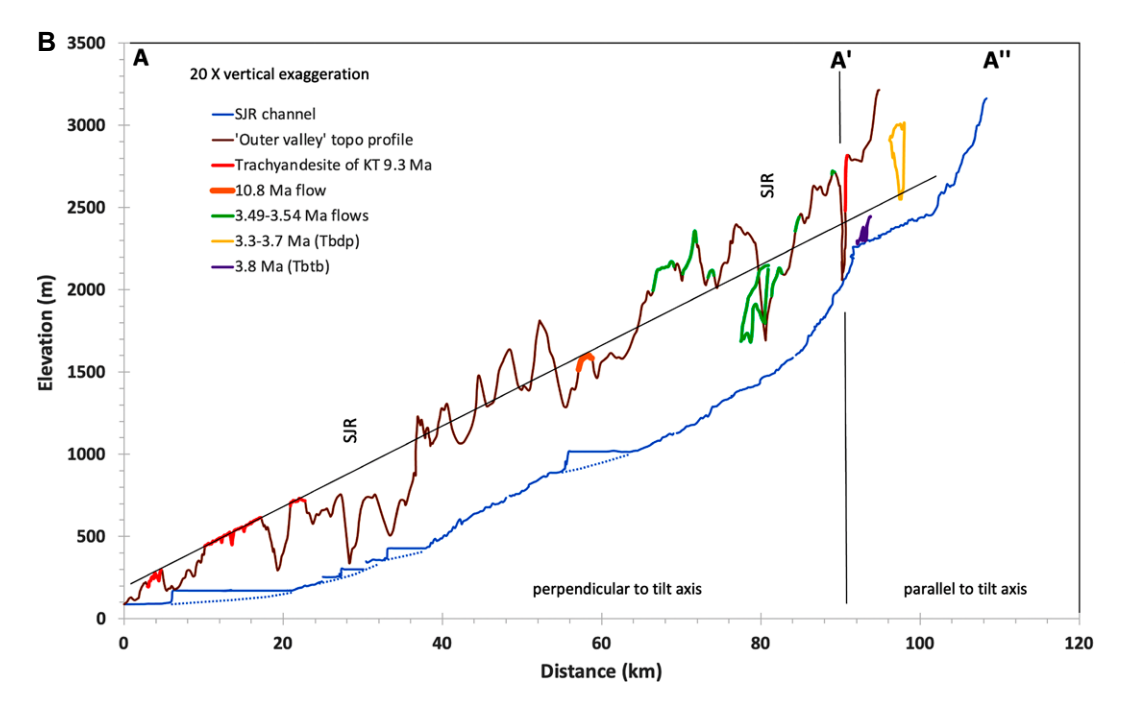


Figure 8. (Continued)

downstream remnants and the vent, and thus limit any cross-range warping to a relatively small amount.

Second, examination of structural and topographic data between the downstream flow remnants and the vent does not indicate any warping. No faults are recognized between the vent and downstream remnants, and the Sierran microplate, which has been translating northwestward for longer than the 9.3 m.y. interval of interest, seems unlikely to have warped along a range-parallel axis. To test this further, we compared topographic profiles along the modern river and along what Matthes (1960) termed the "outer valley." He divided the floor of the San Joaquin drainage into an inner gorge, which he considered to have been carved during the Pleistocene, and the "outer valley," which is a broad paleovalley floor of relatively low relief that he attributed to the Pliocene. Although Matthes' chronology was too young (working before radiometric chronology was available), subsequent work has supported his conceptual model. His "outer valley" is dotted with small lava flows that mostly date to the Pliocene but some to the late Miocene (Dalrymple, 1963; Hildreth and Fierstein, 2016; USGS Menlo Park Ar geochronology laboratory work in progress). Preservation of numerous lava flows (10.8-3.3 Ma) on the paleovalley surface near the inner-gorge rim demonstrates that the paleovalley floor has not been extensively eroded since the Miocene. If the range block had been warped since 9.3 Ma, then the well-preserved valley floor should exhibit a convex-up profile.

Figure 8 shows the profiles for the modern river and for the outer valley. Note that the profile first ascends the south side of the San Joaquin River in order to pass through the remnants of the Trachyandesite of Kennedy Table flow and then crosses to the north side in order to go through the Tertiary lava flows. Finally, it crosses again to the southeast side in order to pass through the Takt vent. The modern profile shows the expected concave-upward shape. In contrast, the outer valley profile is relatively linear. The 10.8 Ma lava flow lies on or slightly below the projection of the trachyandesite flows. It is about halfway between the tilted flow remnants at the range front and their vent, so if there had been any pronounced warping of the range block, it should lie above the projection, which it does not. The linearity of the Miocene profile may be because, at that time, the headwaters of the San Joaquin lay far to the northeast, on the eastern side of the present Sierra crest (Huber, 1981). Rivers are normally strongly convex only near their headwaters, and thus during the Miocene, this portion of the San Joaquin River may have constituted the lower-middle reach, which would not be expected to exhibit much convexity. The parallelism between the projected gradient and the San Joaquin channel reach upstream from A' supports this interpretation.

In summary, the Miocene–Pliocene outer valley, in which erosion has been minimal enough to preserve lava flows from these periods, exhibits a relatively linear profile with no hint of convex-up warping. The paleovalley appears to be on, or close to, the grade of the downstream remnants of the Trachyandesite of Kennedy Table, and a mild concave-up profile would be required to match up with the vent elevation for the flow. These observations are quite inconsistent with the hypothesis of significant convex-up warping. We note that in a similar situation in the northern Sierra Nevada, Wakabayashi and Sawyer (2000) inferred several hundred meters of elevation reduction of the crest along en-echelon strands of the Frontal fault system that cross the crest. Similar deformation cannot be ruled out for the San Joaquin drainage, but the complete lack of mapped faults in suitable positions argues against this interpretation.

At 91 km, the projection line for the channel profile makes an approximate 90° bend to follow the San Joaquin River where it turns from northeast to northwest. The lower section (A-A') is approximately perpendicular to the axis of tilting of the range, while the upper one (A'-A") is approximately parallel to the axis. This turn corresponds closely with the upper limit of post-Pliocene incision of the inner gorge. Shortly above this inflection point, the Basalt of The Buttresses (Tbtb) lava flows, dated to 3.8 Ma (Hildreth and Fierstein, 2016), descend to present-day river level, indicating minimal incision of the upper Middle Fork since the middle Pliocene. The observation that the portion of the San Joaquin River perpendicular to the tilt axis, and thus maximally tilted, has been strongly incised, but the portion parallel to the axis, and thus untilted, has been minimally incised corroborates range-block tilting as the reason for the difference in gradients of the Miocene and modern river channels near the range front. As stated above in discussion of the vent intrusion, most of the incision of the south-flowing reach of the Middle Fork took place between 9.3 and 3.8 Ma. The headward-advancing knickpoint of the inner gorge has now reached the intrusion but remains 3 km south of the Buttresses (Fig. 8).

Comparison with Independent Tilt Estimates

Several other studies have attempted to estimate tilting of the Sierra Nevada block in the vicinity of our study area. (We note that since the geologic histories of the northern and southern ends of the Sierra Nevada are distinct from the central section, our tilt analysis should not be casually extrapolated to those portions of the range.) Unruh (1991) attributed the increase with increasing geological age of the dips of sedimentary units prograding from the block into the Central Valley basin to progressive tilting of the block. For the San Joaquin River area, he obtained dips for Miocene units of 1.26° and 1.5°. Averaging these and subtracting a depositional dip of 0.06°, based on the modern San Joaquin River at the hinge line (discussed above), yield a tilt estimate of 1.3°, which is similar to, but somewhat larger than, ours.

McPhillips and Brandon (2012) employed inversion of thermochronologic data to estimate Sierra Nevada tilting. The San Joaquin River is approximately in the middle of the section of the Sierra Nevada over which their data extended. Their data analysis did support tilting, and accompanying erosion of the range block, in the late Cenozoic. They estimated $1.15^{\circ} \pm 0.35^{\circ}$ degree of tilting since the middle Miocene. This agrees within uncertainty with the 1.22° tilt estimate of Huber (1981) and the 1.07° from this study. McPhillips and Brandon's conclusion is particularly significant with regard to the criticism of rigid-block tilting because their data are in considerable part from near the crest of the range and thus show that the tilting was not confined to the far western margin where Huber performed his study.

As described above, Gabet (2014) criticized the conclusions of Huber (1981) on the basis that only qualitative methods were used to estimate the Miocene river gradient. Gabet (2014) tested Huber's gradient estimate by performing clast-size measurements at Table Mountain. His analysis of those data indicated a depositional slope of 0.05° to 0.29°, which is consistent with our depositional slope value of 0.23° from the meander-tilt analysis, but he based this on a

single sediment sample, limiting confidence in the result.

SUMMARY

We identified the source vent for the Trachyandesite of Kennedy Table at the headwaters of the San Joaquin River and used 40Ar/39Ar to date the eruption to 9.3 Ma. Our topographic analysis of the Table Mountain and McKenzie Table fossil meanders of the Miocene San Joaquin River demonstrated that their original landscape-scale dip was 0.46°, similar to the adjacent modern San Joaquin River, and that they have been tilted down to the west (azimuth of tilt 220°) by 1.07° since 9.3 Ma. This tilt value is a little smaller than that of Huber (1981): 1.22°. The upstream projection of the modern gradient of the trachyandesite flow falls well below the vent elevation at the crest, and the paleovalley floor has a linear profile, indicating that the central Sierra Nevada block has not undergone significant convex warping associated with the tilting. Huber (1981) estimated 2.1 km of uplift of the Sierran crest at the headwaters of the San Joaquin River; our estimates of 1.9-2.1 km of uplift are similar. Our confirmation of Huber's assumptions regarding initial river gradient and rigid-block tilting make his case for ~2 km of crestal uplift a very strong one.

Our estimate of Sierra Nevada block tilt can be compared with independent estimates based on tilting of sedimentary strata in the eastern San Joaquin Valley by Unruh (1991), which yielded $\sim 1.3^{\circ}$ of tilt, and those based on inversion of thermochronological data from the Sierra block by McPhillips and Brandon (2012), which indicated $\sim 1.15^{\circ}$ of tilting. These are similar to our value of 1.07° . The convergence of all these lines of evidence confirms Huber's finding of $1.0^{\circ}-1.2^{\circ}$ of tilt of the central Sierra Nevada block and ~ 2 km of uplift of the crest in this region since 9.3 Ma.

ACKNOWLEDGMENTS

We are pleased to add to the admirable analysis published by King Huber (1981). When Hildreth and Fierstein identified the vent and correlated the lavas a decade ago, they thought it was "no big deal" because the analysis essentially supported Huber. They are grateful to Fred Phillips for pointing out that many in the tectonics and geomorphology communities would indeed be interested. Thanks go to Larry Schemel, Cindy and Bart Topping, and Ed Fadeley for access to Kennedy and Bug Tables, and to the Sierra Foothills Conservancy for access to McKenzie Table and for their work in defending the landscape. Thanks also go to Bob Drake, Jack Fulton, and Paty Sruoga for joining us in the field. Detailed reviews by Charlie Bacon, Greg Stock, Craig Jones, John Wakabayashi, and Emmanuel Gabet improved our presentation. F.M. Phillips' contribution was supported by National Science Foundation grant EAR-1516680.

REFERENCES CITED

- Bateman, P.C., and Busacca, A.J., 1982, Geologic Map of the Millerton Lake Quadrangle, West- Central Sierra Nevada, California: U.S. Geological Survey Geologic Quadrangle Map GQ-1548, scale 1:62,500, https://doi.org/10.3133/gq1548.
- Bateman, P.C., and Eaton, G.P., 1967, Sierra Nevada Batholith: Science, v. 158, p. 1407–1417, https://doi. org/10.1126/science.158.3807.1407.
- Bateman, P.C., and Wahrhaftig, C.A., 1966, Geology of the Sierra Nevada, in Bailey, E.H., ed., Geology of Northern California: California Division of Mines and Geology Bulletin 190, p. 107–172.
- Cassel, E.J., Graham, S.A., and Chamberlain, C.P., 2009, Cenozoic tectonic and topographic evolution of the northern Sierra Nevada, California, through stable isotope paleoaltimetry in volcanic glass: Geology, v. 37, p. 547–550, https://doi.org/10.1130/G25572A.1.
- Cecil, M.R., Ducea, M.N., Reiners, P.W., and Chase, C.G., 2006, Cenozoic exhumation of the northern Sierra Nevada, California, from (U-Th)/He thermochronology: Geological Society of America Bulletin, v. 118, p. 1481–1488, https://doi.org/10.1130/B25876.1.
- Chamberlain, C.P., Mix, H.T., Mulch, A., Hren, M.T., Kent-Corson, M.L., Davis, S.J., Horton, T.W., and Graham, S.A., 2012, The Cenozoic climatic and topographic evolution of the western North American cordillera: American Journal of Science, v. 312, p. 213–262, https://doi.org/10.2475/02.2012.05.
- Christensen, M.N., 1966, Late Cenozoic crustal movements in the Sierra Nevada of California: Geological Society of America Bulletin, v. 77, p. 163–182, https://doi. org/10.1130/0016-7606(1966)77[163:LCCMIT]2.0 .CO:2.
- Clark M.K., Maheo G., Saleeby J., and Farley K.A., 2005, The non-equilibrium landscape of the southern Sierra Nevada, California: GSA Today, v. 15, no. 9, p. 4–10, https://doi.org/10:1130/1052–5173(2005)015<4:TNE LOT>2.0.CO;2.
- Dalrymple, G.B., 1963, Potassium-argon dates of some Cenozoic rocks of the Sierra Nevada: Geological Society of America Bulletin, v. 74, p. 379–390, https:// doi.org/10.1130/0016-7606(1963)74[379:PDOSCV]2 0.CO:2.
- Ducea, M.N., and Saleeby, J.B., 1996, Buoyancy sources for a large, unrooted mountain range, the Sierra Nevada, California: Evidence from xenolith thermobarometry: Journal of Geophysical Research, v. 101, p. 8229–8244, https://doi.org/10.1029/95JB03452.
- Fleck, R.J., Calvert, A.T., Coble, M.A., Wooden, J.L., Hodges, K., Hayden, L.A., van Soest, M.C., du Bray, E.A., and John, D.A., 2019, Characterization of the rhyolite of Bodie Hills and ⁴⁰Ar/³⁹Ar intercalibration with Ar mineral standards: Chemical Geology, v. 525, p. 282–302, https://doi.org/10.1016/j.chemgeo.2019.07.022.
- Gabet, E.J., 2014, Late Cenozoic uplift of the Sierra Nevada, California? A critical analysis of the geomorphic evidence: American Journal of Science, v. 314, p. 1224– 1257, https://doi.org/10.2475/08.2014.03.
- Gilbert, C.M., Christensen, M.N., Al-Rawi, Y., and Lajoie, K.R., 1968, Structural and volcanic history of Mono Basin, California-Nevada, in Coats, R.R., Hay, R.L., and Anderson, C.A., eds., Studies in Volcanology: Geological Society of America Memoir 116, p. 275–331, https://doi.org/10.1130/MEM116-p275.
- Henry, C.D., Hinz, N.H., Faulds, J.E., Colgan, J.P., John, D.A., Brooks, E.R., Cassel, E.J., Garside, L.J., Davis, D.A., and Castor, S.B., 2012, Eocene–early Miocene paleotopography of the Sierra Nevada–Great Basin–Nevadaplano based on widespread ash-flow tuffs and paleovalleys: Geosphere, v. 8, p. 1–27, https://doi.org/10.1130/GES00727.1.
- Hildreth, W., and Fierstein, J., 2016, Eruptive History of Mammoth Mountain and its Mafic Periphery, California: U.S. Geological Survey Professional Paper 1812, 128 p., geologic map scale 1:24,000, https://doi .org/10.3133/pp1812.
- House, M.A., Wernicke, B.P., and Farley, K.A., 1998, Dating topographic uplift of the Sierra Nevada, California, using apatite (U-Th)/He ages: Nature, v. 396, p. 66–69, https://doi.org/10.1038/23926.

- Hren, M.T., Pagani, M., Erwin, D.M., and Brandon, M., 2010, Biomarker reconstruction of the early Eocene paleotopography and paleoclimate of the northern Sierra Nevada: Geology, v. 38, no. 1, p. 7–10, https://doi .org/10.1130/G30215.1.
- Huber, N.K., 1981, Amount and Timing of Late Cenozoic Uplift and Tilt of the Central Sierra Nevada, California—Evidence from the Upper San Joaquin River Basin: U.S. Geological Survey Professional Paper 1197, 28 p., https://doi.org/10.3133/pp1197.
- Huber, N.K., 1990, The late Cenozoic evolution of the Tuolumne River, central Sierra Nevada, California: Geological Society of America Bulletin, v. 102, p. 102–115, https://doi.org/10.1130/0016-7606(1990)102<0102:TLCEOT>2.3.CO;2.
- Janda, R.J., 1966, Pleistocene History and Hydrology of the Upper San Joaquin River, California [Ph.D. dissertation]: Berkeley, California, University of California, 425 p.
- Jayko, A.S., 2009, The Mono Arch, eastern Sierra region, California: Dynamic topography associated with upper-mantle upwelling?: International Geology Review, v. 51, p. 702–722, https://doi .org/10.1080/00206810902880271.
- Jones, C.H., Farmer, G.L., and Unruh, J., 2004, Tectonics of Pliocene removal of lithosphere of the Sierra Nevada, California: Geological Society of America Bulletin, v. 116, p. 1408–1422, https://doi.org/10.1130/B25397.1.
- Le Conte, J., 1886, A post-Tertiary elevation of the Sierra Nevada shown by the river beds: American Journal of Science, ser. 3d, v. 32, p. 167–181.
- Le Pourhiet, L., Gurnisa, M., and Saleeby, J., 2006, Mantle instability beneath the Sierra Nevada mountains in California and Death Valley extension: Earth and Planetary Science Letters, v. 251, p. 104–119, https://doi .org/10.1016/j.epsl.2006.08.028.
- Leopold, L.B., and Wolman, M.G., 1957, River Channel Patterns: Braided, Meandering, and Straight: U.S. Geological Survey Professional Paper 282-B, p. 39–85, https://doi.org/10.3133/pp282B.
- Lindgren, W., 1911, The Tertiary Gravels of the Sierra Nevada: U.S. Geological Survey Professional Paper 73, 226 p., https://doi.org/10.3133/pp73.
- Macdonald, G.A., 1941, Reconnaissance Geologic Map of the Western Part of the Sierra Nevada between the Kings & San Joaquin Rivers, California: University of California Publications in Geological Sciences 26, no. 2, p. 215–286; map scale 1:62,500.

- Martel, S.J., Stock, G.M., and Ito, G., 2014, Mechanics of relative and absolute displacements across normal faults, and implications for uplift and subsidence along the eastern escarpment of the Sierra Nevada, California: Geosphere, v. 10, p. 243–263, https://doi.org/10.1130/GES00968.1.
- Matthes, F.E., 1960, Reconnaissance of the Geomorphology and Glacial Geology of the San Joaquin Basin, Sierra Nevada, California (prepared posthumously by Fritiof Fryxell): U.S. Geological Survey Professional Paper 329, 62 p., https://doi.org/10.3133/pp329.
- Matthes, F.E., 1965, Glacial Reconnaissance of Sequoia National Park, California: Characteristics and Distribution of the Ancient Glaciers in the Most Southerly National Park of the Sierra Nevada (prepared posthumously by Fritiof Fryxell): U.S. Geological Survey Professional Paper 504-A, 58 p., https://doi.org/10.3133/pp504A.
- McPhillips, D., and Brandon, M.T., 2012, Topographic evolution of the Sierra Nevada measured directly by inversion of low-temperature thermochronology: American Journal of Science, v. 312, p. 90–116, https://doi .org/10.2475/02.2012.02.
- Mix, H.T., Caves Rugenstein, J.K., Reilly, S.P., Ritch, A.J., Winnick, M.J., Kukla, T., and Chamberlain, C.P., 2019, Atmospheric flow deflection in the late Cenozoic Sierra Nevada: Earth and Planetary Science Letters, v. 518, p. 76–85, https://doi.org/10.1016/j.epsl.2019.04.050.
- Mix, H.T., Ibarra, D.E., Mulch, A., Graham, S.A., and Chamberlain, C.P., 2016, A hot and high Eocene Sierra Nevada: Geological Society of America Bulletin, v. 128, p. 531–542, https://doi.org/10.1130/B31294.1.
- Saleeby, J.B., Ducea, M.N., Busby, C., Nadin, E., and Whetmore, P.H., 2008, Chronology of pluton emplacement and regional deformation in the southern Sierra Nevada Batholith, California, in Wright, J.E., and Shervais, J.W., eds., Ophiolites, Arcs, and Batholiths: Geological Society of America Special Paper 438, p. 397–428, https://doi.org/10.1130/2008.2438(14).
- Sharman, G.R., Graham, S.A., Grove, M., Kimbrough, D.L., and Wright, J.E., 2015, Detrital zircon provenance of the Late Cretaceous–Eocene California forearc: Influence of Laramide low-angle subduction on sediment dispersal and paleogeography: Geological Society of America Bulletin, v. 127, p. 38–60, https://doi .org/10.1130/B31065.1.
- Small, E.E., and Anderson, R.S., 1995, Geomorphically driven late Cenozoic rock uplift in the Sierra Nevada, California: Science, v. 270, no. 5234, p. 277–281, https://doi.org/10.1126/science.270.5234.277.

- Stock, G.M., Anderson, R.S., and Finkel, R.C., 2004, Pace of landscape evolution in the Sierra Nevada, California, revealed by cosmogenic dating of cave sediments: Geology, v. 32, p. 193–196, https://doi.org/10.1130/ G20197.1.
- Thompson, G.A., and Parsons, T., 2009, Can footwall unloading explain the late Cenozoic uplift of the Sierra Nevada crest?: International Geology Review, v. 51, p. 986–993, https://doi.org/10.1080/00206810903059156.
- Unruh, J.R., 1991, The uplift of the Sierra Nevada and implications for late Cenozoic epeirogeny in the western Cordillera: Geological Society of America Bulletin, v. 103, p. 1395–1404, https://doi.org/10.1130/0016-7606(1991)103<1395:TUOTSN>2.3.CO;2.
- Wahrhaftig, C.A., 1965, Stepped topography of the southern Sierra Nevada, California: Geological Society of America Bulletin, v. 76, p. 1165–1190, https://doi.org/10.1130/0016-7606(1965)76[1165:STOTSS]2.0 CO:2
- Wakabayashi, J., 2013, Paleochannels, stream incision, erosion, topographic evolution, and alternative explanations of paleoaltimetry, Sierra Nevada, California: Geosphere, v. 9, no. 2, p. 191–215, https://doi.org/10.1130/GES00814.1.
- Wakabayashi, J., and Sawyer, T.L., 2000, Neotectonics of the Sierra Nevada and the Sierra Nevada–Basin and Range transition, California, with field trip stop descriptions for the northeastern Sierra Nevada, in Brooks, E.R., and Dida, L.T., eds., Field Guide to the Geology and Tectonics of the Northern Sierra Nevada: California Division of Mines Geology Special Publication 122, p. 173–212.
- Wernicke, B., Clayton, R., Ducea, M., Jones, C.H., Park, S., Ruppert, S., Saleeby, J., Snow, J.K., Squires, L., Fliedner, M., Jiracek, G., Keller, R., Klemperer, S., Luetgert, J., Malin, P., Miller, K., Mooney, W., Oliver, H., and Phinney, R., 1996, Origins of high mountains in the continents: The southern Sierra Nevada: Science, v. 271, p. 190–193, https://doi.org/10.1126/science.271.5246.190.
- Zhou, Q., and Liu, L., 2019, Topographic evolution of the western United States since the early Miocene: Earth and Planetary Science Letters, v. 514, p. 1–12, https://doi.org/10.1016/j.epsl.2019.02.029.

SCIENCE EDITOR: BRAD S. SINGER

Manuscript Received 16 March 2021 Revised Manuscript Received 28 May 2021 Manuscript Accepted 28 June 2021

Printed in the USA